Three-Wave Interaction in a Beam-Plasma System

by

H. J. Hopman

NASA Grant NGL 05-020-176

SU-IPR Report No. 402

December 1970

INSTITUTE FOR PLASMA RESEARCH
STANFORD UNIVERSITY, STANFORD, CALIFORNIA

THREE-WAVE INTERACTION IN A BEAM-PLASMA SYSTEM

by

H. J. Hopman

NASA Grant NGL 05-020-176

SU-IPR Report No. 402

December 1970

Institute for Plasma Research
Stanford University
Stanford, California

THREE-WAVE INTERACTION IN A BEAM-PLASMA SYSTEM *

by

H. J. Hopman†

Institute for Plasma Research
Stanford University
Stanford, California

ABSTRACT

The coupling coefficient for nonlinear three-wave interaction is derived for the case of a cylindrical plasma column penetrated by an electron beam. The parametric growth rate of two plasma waves is calculated, assuming that a negative energy wave on the beam satisfies appropriate synchronism conditions with them and acts as a pump wave. A beam-plasma experiment is described in which three-wave coupling has been observed between two beam waves and a low frequency plasma wave. All three waves grow in space, with a growth rate of the order of one tenth of the wave number of the beam waves.

---

* Work supported by the National Aeronautics and Space Administration.

† On leave from the FOM Institute for Atomic and Molecular Physics, Amsterdam, The Netherlands.

CONTENTS

LIST OF FIGURES

1. INTRODUCTION

Since about 1960, a considerable amount of research has been carried out on linear two-wave interaction, particularly on the unstable interaction between positive and negative energy waves which occurs in a beam-plasma system [Briggs 1964, Hopman 1969]. As early as 1962, Sturrock pointed out that the nonlinear case of three-wave interaction can be unstable in such a way that all three interacting waves have growing amplitudes, and that just as in the unstable case of two-wave coupling, this is only possible when a negative energy wave is involved. The phenomenon is easily demonstrated by means of the conservation relations that hold for three-wave interaction, i.e. the so-called Manley-Rowe relations. When the three interacting waves fulfill resonant conditions for their frequencies and wavenumbers

$$\omega_\alpha = \omega_\beta + \omega_\gamma \ , \quad \underset{\sim}{k}_\alpha = \underset{\sim}{k}_\beta + \underset{\sim}{k}_\gamma \ , \tag{1}$$

where all frequencies are positive, the Manley-Rowe relations say that

$$\frac{\partial}{\partial t}\left(\frac{U_\alpha}{\omega_\alpha}\right) = -\frac{\partial}{\partial t}\left(\frac{U_\beta}{\omega_\beta}\right) = -\frac{\partial}{\partial t}\left(\frac{U_\gamma}{\omega_\gamma}\right) . \tag{2}$$

Consequently, when the energy, U_α, of wave α is negative, all three wave amplitudes can grow (or decay) in time.

When only positive energy waves are interacting, there is a periodic exchange of energy [Sagdeev and Galeev, 1969], leading to a growth of one or of two of the interacting waves for a limited time. When the highest frequency wave is a negative energy wave, growth again occurs only within a limited time, but in this case the amplitudes of all three waves tend to infinity in this time. The growth must therefore be faster than the exponential growth that occurs due to two-wave coupling. This characteristic behavior of three-wave interaction is now generally referred to as "explosive instability" [Hasegawa et al., 1969; Fukai et al.,1969].

In this report, the strength of the three-wave coupling that results from a weak nonlinearity of the Vlasov equation is examined. The analysis follows closely the treatment of Dysthe [1970], and is carried out for

a cylindrical plasma column in an infinite magnetic field, taking as a boundary condition that the wave potential is zero outside the plasma. This is equivalent to studying a plasma-filled waveguide. By comparing the results for the infinite plasma [Dysthe, 1970] and the bounded plasma column, it is found that the expressions for the time dependences of the wave amplitudes are identical, a conclusion that can also be extended to surface waves on a plasma column in vacuum when the dc magnetic field is absent. The basic theory up to this point is given in Sections 2 and 3.

Due to the shape of their dispersion characteristic, three quasi-static plasma waves can never satisfy the resonance conditions of Eq. (1) in a one-component plasma, so three-wave interaction is impossible. When two components are present, interaction is possible, however. Examples are an ion-electron plasma, or a beam-plasma system. In the former case, the decay of a Langmuir wave into a lower frequency Langmuir wave and an ion acoustic wave has attracted much attention. The latter case has only appeared in discussions recently, with special focus on the participation of a negative energy beam wave. Wilhelmsson [1969] reported computer calculations on the time behavior of the wave amplitudes, demonstrating the explosive growth, while Pham-Tu-Manh [1969] has described experimental work.

The present report gives calculated growth rates for the nonlinear instability which occurs when a negative energy wave interacts with two plasma waves that are propagating in opposite directions. This topic is treated in Section 4. So far, this interaction has not been studied in detail in our experimental work, which has been concerned with instabilities at low frequencies, in particular near the ion plasma frequency. Nonlinear interactions in this frequency range are treated in Section 4, and preliminary results are described in Section 5 which suggest that we may have observed them experimentally.

2. BASIC EQUATIONS

To obtain the nonlinear growth rate due to wave-wave coupling, we determine first the linear dispersion of the modes separately. After that, the nonlinear term is evaluated by considering the interaction between the modes.

We start with the Vlasov equation for each plasma component

$$\left\{ \frac{\partial}{\partial t} + \underset{\sim}{v} \cdot \nabla + \frac{e_j}{m_j} \left(\underset{\sim}{E} + \underset{\sim}{v} \times \underset{\sim}{B} \right) \cdot \nabla_v \right\} f_j = 0 \ , \tag{3}$$

and the Poisson equation

$$\nabla \cdot \underset{\sim}{E} = \frac{1}{\epsilon_0} \sum_j n_{0j} e_j \int_{-\infty}^{\infty} f_j \, d\underset{\sim}{v} \ . \tag{4}$$

The different particle species, j, may be plasma ions (i), plasma electrons (e), and beam electrons (b). The velocity distribution functions, f_j, are normalized to unity. Charge neutrality demands that integration over unit volume should yield

$$\iint n_{0i} f_i \, d\underset{\sim}{v} \, d\underset{\sim}{x} = \iint \left[n_{0e} f_e + n_{0b} f_b \right] d\underset{\sim}{v} \, d\underset{\sim}{x} = n_0 \ . \tag{5}$$

We shall restrict the analysis to slow waves, so that the quasi-static approximation can be made. This implies that the electric field is derivable from a potential ($\underset{\sim}{E} = - \nabla V$). Next, we divide the distribution function into slowly and rapidly fluctuating parts with respect to the propagating waves

$$f_j = f_{0j}(\underset{\sim}{v},\underset{\sim}{x},t) + f_{1j}(\underset{\sim}{v},\underset{\sim}{x},t) \ . \tag{6}$$

Linearization of Eq. (3), neglecting the space-time dependence of f_{0j}, then gives to first order

$$\left\{ \frac{\partial}{\partial t} + \underset{\sim}{v} \cdot \nabla + \frac{e_j}{m_j} \underset{\sim}{v} \times \underset{\sim}{B}_0 \cdot \nabla_v \right\} f_{1j} - \frac{e_j}{m_j} \nabla V \cdot \nabla_v f_{0j} = 0 \ . \tag{7}$$

We write V as a sum over the normal modes that propagate in the plasma in the z-direction, which is aligned with the axis of the plasma column.

$$V(\underset{\sim}{x},t) = \sum_{\alpha=-\infty}^{+\infty} V_\alpha(\underset{\sim}{x},t) \exp i(\omega_\alpha t - k_\alpha z) \ . \qquad (8)$$

Just like f_{0j}, the normal mode amplitude $V_\alpha(\underset{\sim}{x},t)$ has a space-time dependence that is slow with respect to $(\omega_\alpha t - k_\alpha z)$. This is neglected in calculating the linear dispersion.

In Eq. (8), we require V to be real quantity. Therefore $V_{-\alpha} = V_\alpha^*$, where $*$ denotes a complex conjugate. The change of sign of α symbolizes the reversal of signs of ω and k. Thus, $\omega_\alpha = -\omega_{-\alpha}$, $k_\alpha = -k_{-\alpha}$.

From Eq. (4) we obtain

$$\nabla V = -i\underset{\sim}{e}_z \sum_\alpha V_\alpha k_\alpha \exp i(\omega_\alpha t - k_\alpha z) \ , \qquad (9)$$

$\underset{\sim}{e}_z$ being the unit vector in the z-direction. The dependence of V_α on the coordinates perpendicular to z is determined by the boundary conditions that are used for a particular case. In the following section, we discuss the particular case of a plasma column filling a waveguide. A strong dc magnetic field, B_0, directed along the column axis inhibits particle motion perpendicular to z. Thus, $\underset{\sim}{v}_\perp \approx 0$, and we will be treating effectively a one-dimensional system.

3. PLASMA COLUMN IN A STRONG MAGNETIC FIELD

3.1. Linear Propagation

With $\underset{\sim}{v}_\perp = 0$, Eqs. (7) and (9) combine to give

$$\left\{\frac{\partial}{\partial t} + v_z \frac{\partial}{\partial z}\right\} f_{1j} + i \frac{e_j}{m_j} \sum_\alpha V_\alpha k_\alpha \frac{\partial f_{0j}}{\partial v_z} \exp i(\omega_\alpha t - k_\alpha z) = 0. \quad (10)$$

Writing v_α for the phase velocity, ω_α / k_α , and integrating Eq. (10), yields

$$f_{1j} = - \frac{e_j}{m_j} \sum_\alpha \frac{V_\alpha \frac{\partial f_{0j}}{\partial v_z}}{v_\alpha - v_z} \exp i(\omega_\alpha t - k_\alpha z) \ . \quad (11)$$

Substitution of Eq. (11) in Eq. (4) yields an equation of the form

$$[\nabla_\perp^2 + p_\alpha^2] V_\alpha = 0 \ , \ -p_\alpha^2 = k_\alpha^2 + \sum_j \omega_{pj}^2 \int \frac{(\partial f_{0j}/\partial v_z) d\underset{\sim}{v}}{v_\alpha - v_z} \ , \quad (12)$$

which has as solution a sum of Bessel function terms $J_m(p_\alpha r)$, exp im θ , and $N_m(p_\alpha r)$ exp im θ , where r and θ are cylindrical polar coordinates. The requirements of a non-infinite solution on the column axis, and a zero at the conducting wall surrounding the plasma at $r = a$, restricts the solution to

$$V_\alpha(r,\theta,z,t) = \hat{V}_{\alpha mn}(z,t) \, J_m(p_\alpha r) \exp(im\theta), \quad p_\alpha a = j_{mn} \ , \quad (13)$$

where j_{mn} is the n^{th} zero of the m^{th} Bessel function, $J_m(p_\alpha r)$, and $\hat{V}_{\alpha mn}$ is the slowly varying amplitude of mode (α,m,n) determined by initial conditions.

Combining Eqs. (12) and (13), we write

$$D_\alpha(\omega,k)\ \hat{V}_{\alpha mn} = \frac{p_\alpha^2+k_\alpha^2\epsilon_\alpha(\omega,k)}{p_\alpha^2+k_\alpha^2}\ \hat{V}_{\alpha mn}$$

$$= \left[1 + \frac{1}{p_\alpha^2+k_\alpha^2}\sum_j \omega_{pj}^2 \int \frac{\partial f_{0j}/\partial v_z}{v_\alpha - v_z}\, d\underline{v}\right] \hat{V}_{\alpha mn} = 0\ . \tag{14}$$

The solution of Eq. (10) is just $D_\alpha(\omega,k) = 0$, and constitutes the dispersion equation for the normal modes α. The quantity $\epsilon_\alpha(\omega,k)$ is the one-dimensional plasma permittivity. An equivalent expression for the plasma dispersion equation is

$$-p_\alpha^2 = k_\alpha^2\,\epsilon_\alpha\ , \tag{15}$$

which is familiar in plasma literature [Trivelpiece, 1967]. The index α attached to D and ϵ indicates that they represent the appropriate expressions for mode α.

3.2. Nonlinear Coupling

The nonlinear equation that describes mode coupling is found by substituting the linear expression for f_{1j}, given by Eq. (6), in the nonlinear term of the full Vlasov equation, and calculating f_{1j} again, correct to second order. This iteration yields

$$\left\{\frac{\partial}{\partial t} + v_z\frac{\partial}{\partial z}\right\} f_{1j} = -i\,\frac{e_j}{m_j}\sum_\alpha V_\alpha k_\alpha \frac{\partial f_{0j}}{\partial v_z}\exp i(\omega_\alpha t - k_\alpha z)$$

$$+ i\,\frac{e_j^2}{m_j^2}\sum_\gamma\sum_\beta k_\beta V_\beta V_\gamma \frac{\partial}{\partial v_z}\left[\frac{\partial f_{0j}/\partial v_z}{v_\gamma - v_z}\right]\exp i[(\omega_\beta+\omega_\gamma)t - (k_\beta+k_\gamma)z]\ . \tag{16}$$

After averaging in space and time, the right-hand side of Eq. (16) still contributes if its rapid space-time variation is equal to that of the left-hand side. We therefore consider the resonant situation

$$\omega_\alpha = \omega_\beta + \omega_\gamma \ , \ k_\alpha = k_\beta + k_\gamma \ , \ m_\alpha = m_\beta + m_\gamma \ , \qquad (17)$$

and retain terms in the double sum that fulfill these conditions, discarding all others. Subsequent integration gives

$$f_{1j} = \left[- \frac{e_j}{m_j} \sum_\alpha \frac{V_\alpha (\partial f_{0j}/\partial v_z)}{v_\alpha - v_z} + \frac{e_j^2}{m_j^2} \sum_\alpha \sum_{\beta+\gamma=\alpha} V_\beta V_\gamma \frac{k_\beta}{k_\alpha (v_\alpha - v_z)} \frac{\partial}{\partial v_z} \left\{ \frac{\partial f_{0j}/\partial v_z}{v_\gamma - v_z} \right\} \right]$$

$$\times \exp i(\omega_\alpha t - k_\alpha z) \ . \qquad (18)$$

The next step is to substitute Eq. (18) in Eq. (4). Because the V's are proportional to $\exp im\theta$, the substitution and application of the condition in Eq. (17) on the azimuthal mode numbers reduces the averaged equations to the form

$$\left\{ \frac{\partial^2}{\partial r^2} + \frac{1}{r} \frac{\partial}{\partial r} - \frac{m_\alpha^2}{r^2} + p_\alpha^2 - \left(p_\alpha^2 + k_\alpha^2 \right) D_\alpha \right\} V_\alpha(r) \qquad (19)$$

$$= \sum_j \frac{\omega_{pj}^2 e_j}{2 m_j} \sum_{\beta+\gamma=\alpha} V_\beta(r) V_\gamma(r) \int \frac{\partial f_{0j}/\partial v_z}{k_\alpha (v_\alpha - v_z)^2} \left[\frac{k_\beta}{v_\gamma - v_z} + \frac{k_\gamma}{v_\beta - v_z} \right] d\underset{\sim}{v}$$

$$= \sum_j \frac{\omega_{pj}^2 e_j}{2 m_j} \sum_{\beta+\gamma=\alpha} J_{m_\beta}(p_\beta r) \, J_{m_\gamma}(p_\gamma r) \, \hat{V}_{\beta m_\beta n_\beta} \, \hat{V}_{\gamma m_\gamma n_\gamma} \int \frac{\left(\partial f_{0j}/\partial v_z \right) d\underset{\sim}{v}}{\prod_\alpha (v_\alpha - v_z)} \ .$$

The term $k_\gamma/(v_\beta - v_z)$ has been added to symmetrize the integrand.

As a solution to Eq. (15), we try

$$V_\alpha(r) = \hat{V}_{\alpha \, m_\alpha n_\alpha} J_{m_\alpha}(j_{m_\alpha n_\alpha} r/a) = \hat{V}_{\alpha m_\alpha n_\alpha} J_{m_\alpha}(p_\alpha r) \ . \qquad (20)$$

Multiplying Eq. (19) by $J_m(j_{m\ell} r/a)$, and making use of the following orthogonality relation for Bessel functions

$$\int_0^a dr\ r\ J_m(j_{mn}\ r/a)\ J_m(j_{m\ell}\ r/a) = \frac{a^2}{2}\ \delta_{n\ell}\left[J'_m(j_{mn})\right]^2$$

$$= \frac{a^2}{2}\ \delta_{n\ell}\ J^2_{m-1}\ (j_{mn})\ , \qquad (21)$$

we obtain

$$D_\alpha\ \hat{V}_{\alpha\ m_\alpha n_\alpha} = \sum_{\beta+\gamma=\alpha} \frac{\Gamma_{\alpha\beta\gamma}\ \hat{V}_{\beta m_\beta n_\beta}\ \hat{V}_{\gamma m_\gamma n_\gamma}\ A_\alpha}{p_\alpha^2 + k_\alpha^2}\ , \qquad (22)$$

where $\Gamma_{\alpha\beta\gamma}$ and A_α are defined by,

$$\Gamma_{\alpha\beta\gamma} = -\sum_j \frac{\omega_{p\gamma}^2\ e_j}{2m_j} \int \frac{(\partial f_{0j}/\partial v_z)\ dv}{\prod_\alpha (v_\alpha - v_z)}\ ,$$

$$A_\alpha = 2\int_0^a dr\ r\ J_{m_\alpha}(p_\alpha r)\ J_{m_\beta}(p_\beta r)\ J_{m_\gamma}(p_\gamma r) \Big/ a^2 J^2_{m_\alpha - 1}\ (p_\alpha a)\ . \qquad (23)$$

As could be expected for waves propagating along a plasma column, the radial dependence of the wave potential is determined by boundary conditions only; there is no restriction on the radial mode numbers, j_{mn}, of the interacting waves. This has been pointed out by Etievant et al. [1967]. However, the amplitude of the nonlinear wave depends on the amount of radial coherence between the modes through Eq. (23). In practical cases, the strongest interaction is to be expected between lower order modes $m_i = 0$ and $p_i = 2.4/a$. Then $J_1^2(j_{01}) = 0.52^2$ and the integral over the triple product of $J_0(pz)$ gives $0.098a^2$ [Fettis, 1957], resulting in $A_\alpha = 0.72$. Except for the amplitude factor, Eq. (22) is precisely what one obtains just by replacing $\nabla_\perp^2$, in Poisson's equation, by $-p_\alpha^2$, as can be done in the linear case. This replacement is, in fact, valid for an infinite plasma.

So far, the slow space-time dependence of the amplitudes, $\hat{V}_i$, has been neglected. However, due to the coupling of mode α to the modes β and γ, there is exchange of energy, and the amplitude V_α will not be constant. The slow space-time variation can be accounted for by means of a method devised by Berk and Book [1969], which replaces the dispersion function, $D_\alpha(\omega,k)$, by an operator $D(\omega - i\frac{\partial}{\partial t}, k + i\frac{\partial}{\partial z}, z, t)$. Using a WKB approach, they proved that this replacement is valid, and leads to the correct dispersion properties for linear waves in an inhomogeneous plasma. The next step is to apply the method to a nonlinear problem. This has been taken by Dysthe [1970] and Dum and Ott [1970], although without proof. Using only the lowest order derivatives, the definition of D is

$$D\left(\omega - i\frac{\partial}{\partial t}, k + i\frac{\partial}{\partial z}, z,t\right) V_\alpha(z,t) = \left\{D_\alpha - i\frac{\partial D_\alpha}{\partial\omega}\frac{\partial}{\partial t} + i\frac{\partial D_\alpha}{\partial k}\frac{\partial}{\partial z} - \frac{i}{2}\frac{\partial^2 D_\alpha}{\partial t\partial\omega} - \frac{i}{2}\frac{\partial^2 D_\alpha}{\partial z\partial k}\right\}\hat{V}_\alpha(z,t) \quad . \tag{24}$$

Applying this operator to Eq. (22), for a homogeneous plasma in which D_α does not depend on z and t explicitly, the result is

$$\left\{D_\alpha - i\frac{\partial D_\alpha}{\partial\omega}\frac{\partial}{\partial t} + i\frac{\partial D_\alpha}{\partial k}\frac{\partial}{\partial z}\right\}\hat{V}_\alpha = \sum_{\beta+\gamma=\alpha}\frac{\Gamma_{\alpha\beta\gamma}\hat{V}_\beta\hat{V}_\gamma A_\alpha}{p_\alpha^2 + k_\alpha^2} \quad . \tag{25}$$

For simplicity, we have dropped the indices m and n from the $\hat{V}$'s.

Next we define the group velocity, $\underset{\sim}{v}_{g\alpha}$, and the linear wave damping, γ_α,

$$\underset{\sim}{v}_{g\alpha} = \left(\frac{d\omega}{d\underset{\sim}{k}}\right)_\alpha = -\frac{\partial D_\alpha/\partial\underset{\sim}{k}}{\partial D_\alpha/\partial\omega}, \quad \gamma_\alpha = i\frac{D_\alpha}{\partial D_\alpha/\partial\omega} \quad . \tag{26}$$

We can then reduce Eq. (25) to

$$\left\{\frac{\partial}{\partial t} + v_{g\alpha}\frac{\partial}{\partial z} + \gamma_\alpha\right\}\hat{V}_\alpha = i\sum_{\beta+\gamma=\alpha}\frac{\Gamma_{\alpha\beta\gamma}\,\hat{V}_\beta\,\hat{V}_\gamma\,A_\alpha}{\left(p_\alpha^2 + k_\alpha^2\right)\left(\partial D_\alpha/\partial\omega\right)} \quad . \tag{27}$$

By analogy, we obtain two further coupled mode equations

$$\left\{\frac{\partial}{\partial t} + v_{g\beta}\frac{\partial}{\partial z} + \gamma_\beta\right\}\hat{V}_\beta = i\sum_{\alpha-\gamma=\beta}\frac{\Gamma_{\alpha\beta\gamma}\,\hat{V}_\alpha\,\hat{V}^*_\gamma\,A_\beta}{\left(p_\beta^2 + k_\beta^2\right)\left(\partial D_\beta/\partial\omega\right)} \quad , \tag{28}$$

$$\left\{\frac{\partial}{\partial t} + v_{g\gamma}\frac{\partial}{\partial z} + \gamma_\gamma\right\}\hat{V}_\gamma = i\sum_{\alpha-\beta=\gamma}\frac{\Gamma_{\alpha\beta\gamma}\,\hat{V}_\alpha\,\hat{V}^*_\beta\,A_\gamma}{\left(p_\gamma^2 + k_\gamma^2\right)\left(\partial D_\gamma/\partial\omega\right)} \quad . \tag{29}$$

Here, we have used the fact that the real part of $\Gamma_{\alpha\beta\gamma}$ is completely symmetric in the indices. It is not affected by a change in the sign of the indices because $\mathrm{Re}\,\Gamma_{\alpha\beta\gamma}$ is a function of the phase velocity $v_\alpha = \omega_\alpha/k_\alpha$. This is not the case for $\mathrm{Im}\,\Gamma_{\alpha\beta\gamma}$, which we neglect. It should be emphasized that Eqs. (27)-(29) only describe the slow space-time behavior of the mode amplitudes, $\hat{V}_i$. The small-signal frequencies and wave numbers are not altered in this treatment.

3.3. Coupling of Waves in Finite and Infinite Plasmas

For comparison with Eq. (27), we give the equivalent mode coupling expression for the case of an infinite, one-dimensional plasma [Dysthe, 1970].

$$\left\{\frac{\partial}{\partial t} + v_{g\alpha\,\mathrm{inf}}\frac{\partial}{\partial z} + \gamma_\alpha\right\}\hat{V}_\alpha = i\sum_{\beta+\gamma=\alpha}\frac{\Gamma_{\alpha\beta\gamma}\,\hat{V}_\beta\,\hat{V}_\gamma}{k_\alpha^2\left(\partial\epsilon_\alpha/\partial\omega\right)} \quad , \tag{30}$$

where the definitions of ϵ_α and D_α are consistent with Eq. (14). This implies

$$\left(p^2 + k^2\right)\frac{\partial D}{\partial\omega} = k^2\frac{\partial\epsilon}{\partial\omega} \quad . \tag{31}$$

Except for the amplitude factor, A_α, which is of order unity, the coupling terms are seen to be identical in the case of a finite plasma column to those for an infinite plasma [Spithas and Manheimer, 1970]. However, the occurrence of the group velocity on the left-hand side causes a great difference between these two physical situations. In an infinite plasma, v_g is determined by the plasma permittivity, ϵ, and we have

$$v_{g\ inf} = -\frac{\partial\epsilon/\partial k}{\partial\epsilon/\partial\omega} . \tag{32}$$

In a finite plasma, v_g is given by Eq. (26), the difference being due to the fact that $\epsilon = 0$ in an infinite plasma, but $\epsilon = -p^2/k^2$ for a plasma-filled waveguide. From the definitions of ϵ and D, and from their magnitudes, we obtain the relation

$$v_g = v_{g\ inf} - \frac{2\epsilon}{k(\partial\epsilon/\partial\omega)} = v_{g\ inf} + \frac{2p^2}{k^3(\partial\epsilon/\partial\omega)} . \tag{33}$$

Writing Eq. (27) in terms of ϵ, we have

$$\left\{\frac{\partial}{\partial t} + \left[v_{g\ inf} + \frac{2p_\alpha^2}{k_\alpha^3(\partial\epsilon_\alpha/\partial\omega)}\right]\frac{\partial}{\partial z} + \gamma_\alpha\right\}\hat{V}_\alpha = i\sum_{\beta+\gamma=\alpha}\frac{\Gamma_{\alpha\beta\gamma}\hat{V}_\beta\hat{V}_\gamma A_\alpha}{k_\alpha^2(\partial\epsilon_\alpha/\partial\omega)} , \tag{34}$$

for the coupled mode expression for a plasma column. The difference with respect to Eq. (30) is now clear. An illustration of the importance of this difference can be given by considering a cold electron plasma. We then have $v_{g\ inf} = 0$, whereas in a finite plasma $v_g = p^2 v_p/(p^2 + k^2)$, where v_p is the phase velocity.

It may be remarked that although the spatial behavior of coupled mode amplitudes is significantly different in a plasma guide and in an infinite plasma, due to the different magnitudes of the group velocity, identical time behavior is found for finite and infinite plasmas. This is due to the fact that $\epsilon(\omega,k)$ is equal to a frequency independent constant, $-p^2/k^2$. Another physical situation where this is true is that of surface waves propagating on a plasma column when a dc magnetic

field is absent. Derivation of the constant in this case is given by Trivelpiece [1967], and the nonlinear coupled-mode equation for surface waves can be written down in analogy to Eq. (34).

3.4. Parametric growth

In addition to the possibility that all three interacting waves will grow in amplitude, when the waves have the correct sign for the wave energy, we may consider the possible occurrence of parametric growth. In parametric growth, it is assumed that one wave is so strong that its space-time variation can be neglected in comparison with that of the other two waves. We take Wave α as being the strong (pump) wave. With $\hat{V}_\alpha$ = constant, we use only Eqs. (28) and (29). Eliminating $\hat{V}_\beta$, we obtain

$$\left\{\frac{\partial}{\partial t} + v_{g\beta}\frac{\partial}{\partial z} + \gamma_\beta\right\}\left\{\frac{\partial}{\partial t} + v_{g\gamma}\frac{\partial}{\partial z} + \gamma_\gamma\right\}\hat{V}_\gamma = 4\,\frac{|\Gamma_{\alpha\beta\gamma}|^2 |\hat{V}_\alpha|^2 A_\gamma A_\beta \hat{V}_\gamma}{\left(p_\beta^2+k_\beta^2\right)\left(p_\gamma^2+k_\gamma^2\right)\frac{\partial D_\beta}{\partial\omega}\frac{\partial D_\gamma}{\partial\omega}}. \qquad (35)$$

Assuming a solution for $\hat{V}_\beta$, $\hat{V}_\gamma$ of the form $\exp(\Omega t - \kappa z)$, where Ω and κ represent the slow space-time dependence of the wave amplitudes, and considering identical radial modes so that we can drop the subscripts from p_i and A_i, we obtain the dispersion relation

$$\left\{\Omega - \kappa v_{g\beta} + \gamma_\beta\right\}\left\{\Omega - \kappa v_{g\gamma} + \gamma_\gamma\right\} = \frac{4A^2|\Gamma_{\alpha\beta\gamma}|^2|\hat{V}_\alpha|^2}{\left(p^2+k_\beta^2\right)\left(p^2+k_\gamma^2\right)\frac{\partial D_\beta}{\partial\omega}\frac{\partial D_\gamma}{\partial\omega}} = \gamma_{\beta\gamma}^2. \qquad (36)$$

Considering only time dependence, we see from Eq. (36) that

$$\Omega = -\left(\frac{\gamma_\beta + \gamma_\gamma}{2}\right) \pm \left(\left(\frac{\gamma_\beta - \gamma_\gamma}{2}\right)^2 + \gamma_{\beta\gamma}^2\right)^{1/2}. \qquad (37)$$

The necessary condition for growth ($\Omega > 0$) is given by

$$\gamma_{\beta\gamma}^2 > \gamma_\beta \gamma_\gamma \ . \tag{38}$$

With no linear damping present, $\gamma_\beta = \gamma_\gamma = 0$. Condition (38) is then satisfied if $\partial D_\beta/\partial\omega$ and $\partial D_\gamma/\partial\omega$ have the same sign.

Considering only spatial dependence, we find from Eq. (36) the necessary condition for spatial growth in the absence of linear damping

$$\frac{\gamma_{\beta\gamma}^2}{v_{g\beta}\, v_{g\gamma}} = \frac{4A^2 \Gamma_{\alpha\beta\gamma}^2 |\hat{V}_\alpha|^2}{\left(p^2+k_\beta^2\right)\left(p^2+k_\gamma^2\right)\frac{\partial D_\beta}{\partial k}\frac{\partial D_\gamma}{\partial k}} > 0 \ , \tag{39}$$

which can be satisfied when $\partial D_\beta/\partial k$ and $\partial D_\gamma/\partial k$ have similar signs.

It should be noted that condition (38) tells us when the system is nonlinearly unstable, but condition (39) says in addition whether the growth is convective or absolute. Absolute growth is obtained when the group velocities of the two waves are opposite in sign, irrespective of the character of the pump wave. However, when $v_{g\beta}\, v_{g\gamma} < 0$, there is still an initial spatial growth, if the system is restricted to a length, L, less than a quarter wavelength

$$L < \frac{\pi}{2\kappa} \ , \tag{40}$$

because the slow spatial behavior is sinusoidal. This is analogous to the situation in a backward wave oscillator. The classification of instabilities due to both two-wave and three-wave coupling has been reviewed by Barnes [1964].

4. APPLICATION TO A COLD BEAM-PLASMA SYSTEM

4.1. Linear and Nonlinear Dispersion

Substitution into the expressions for $\Gamma_{\alpha\beta\gamma}$ and D_α [Eqs. (14) and (23)] of a δ-function velocity distribution,

$$f_{0j} = \delta(v_z - v_{0j})\, \delta(v_r)\, \delta(v_\theta) , \tag{41}$$

for each of the plasma components results in

$$D_\alpha = 1 - \frac{1}{p^2 + k_\alpha^2} \sum_j \frac{\omega_{pj}^2}{(v_\alpha - v_{0j})^2} , \tag{42}$$

$$\Gamma_{\alpha\beta\gamma} = \sum_j \frac{e_j \omega_{pj}^2}{2m_j} \prod_\alpha \left(\frac{1}{v_\alpha - v_{0j}}\right) \sum_\alpha \left(\frac{1}{v_\alpha - v_{0j}}\right). \tag{43}$$

The experiment to be discussed in Section 5 provides the possibility of studying the interaction between modes on an electron beam and in a beam-produced plasma. Neglecting the positive ions, $\Gamma_{\alpha\beta\gamma}$ then becomes

$$\Gamma_{\alpha\beta\gamma} = -\frac{e\omega_{pe}^2}{2m}\left[\prod_\alpha \left(\frac{1}{v_\alpha}\right)\sum_\alpha \left(\frac{1}{v_\alpha}\right) + \frac{\omega_{pb}^2}{\omega_{pe}^2} \prod_\alpha \left(\frac{1}{v_\alpha - v_{0b}}\right)\sum_\alpha \left(\frac{1}{v_\alpha - v_{0b}}\right)\right] , \tag{44}$$

where v_{0b} is the dc velocity of the electron beam. Moreover, in the experiment it is possible to apply rf modulation to the electron beam, and to observe wave growth with distance from the gun. The only term of interest on the left-hand side of Eq. (27) is then $v_{g\alpha}\partial\hat{V}_\alpha/\partial z$, describing the spatial growth. For the δ-function distribution of Eq. (41), Eqs. (28) and (36) reduce to

$$\frac{\partial \hat{V}_\beta}{\partial z} = i\, A\Gamma_{\alpha\beta\gamma} \hat{V}_\gamma^*\, \hat{V}_\alpha / \Delta_\beta , \tag{45}$$

$$\kappa = A|\Gamma_{\alpha\beta\gamma}||\hat{V}_\alpha|\Big/\left(-\Delta_\beta\,\Delta_\gamma\right)^{1/2} \quad , \tag{46}$$

where it has been assumed that Wave α is the pump wave, and we have $\gamma_\beta = \gamma_\gamma = 0$. The quantity Δ_β is defined by

$$\Delta_\beta = -\frac{1}{2}\left(p^2 + k_\beta^2\right)\frac{\partial D_\beta}{\partial k}$$

$$= \frac{1}{k_\beta\left(p^2 + k_\beta^2\right)} \sum_j \omega_{pj}^2 \frac{v_\beta p^2 + v_{0j} k_\beta^2}{\left(v_\beta - v_{0j}\right)^3} \quad . \tag{47}$$

Equation (45) is similar to a result obtained earlier by Etievant et al. [1967] for an infinite plasma, the only modification being the factor A which is of order unity.

Equation (46) shows that $\kappa \propto |\Gamma_{\alpha\beta\gamma}|$. The sign of e_j in $\Gamma_{\alpha\beta\gamma}$ consequently has no influence on the type of growth. It is, of course, natural that there should be no difference when considering waves propagating on positive or on negative particle beams. We observe, however, that the nonlinear growth rate $\propto 1/m$, and is thus much smaller for waves propagated on ion streams.

4.2. Linear Stability Characteristics

In order to observe nonlinear instability in a beam-plasma experiment, it is highly desirable to have the system linearly stable. The condition for linear stability is obtained from Eq. (42) as

$$\frac{pv_{0b}}{\omega_{pe}} > \left[1 + \left(\frac{\omega_{pb}}{\omega_{pe}}\right)^{2/3}\right]^{3/2} \quad . \tag{48}$$

We note that this condition can only be fulfilled in a bounded plasma, where p is fixed by the boundary conditions. The origin of Eq. (48) can be appreciated by taking a simplified model in which the beam and plasma modes are considered to be independent. This means that Eq. (42) holds for plasma and beam separately, giving the dispersion equations

$$1 - \frac{k^2 \omega_{pe}^2}{\omega^2(p^2 + k^2)} = 0 \ , \ 1 - \frac{k^2 \omega_{pb}^2}{(\omega - kv_{0b})^2(p^2 + k^2)} = 0 \ . \qquad (49)$$

From here on, for convenience, we will simply write v_0 for v_{0b}. In Fig. 1 we illustrate the dispersion of the beam and plasma waves. The system is stable when the beam and plasma branches do not intersect, i.e. for $k \to 0$ we require $\lim (d\omega/dk)_b > \lim (d\omega/dk)_e$. Now in this region the waves are nondispersive, and Eq. (49) reduces to

$$p\omega \approx \pm k\omega_{pe} \ , \ p\omega \approx pkv_0 - k\omega_{pb} \ , \qquad (50)$$

where the second expression holds for the slow beam wave. The first expression is very useful for determining the plasma density [Trivelpiece, 1967]. Using Eq. (50), an approximate condition on the group velocities is

$$\frac{pv_0}{\omega_{pe}} > 1 + \frac{\omega_{pb}}{\omega_{pe}} \ , \qquad (51)$$

which is somewhat less restrictive than the more correct form of Eq. (48).

Having illustrated that parameters can be chosen for which small-signal growth is precluded, we now consider the question of synchronism. Suitable conditions for nonlinear interaction, such that

$$\omega_\alpha = \omega_\beta + \omega_\gamma \ , \ k_\alpha = k_\beta + k_\gamma \ , \qquad (52)$$

are indicated in Fig. 1 by a parallelogram. It is clear from the figure that the possibility of three-wave interaction is restricted to frequencies below $2\omega_{pe}$. When Wave α is the beam wave, we have

$$\omega_\alpha < 2\omega_{pe} \ , \quad \omega_\beta, \omega_\gamma < \omega_{pe} \ . \qquad (53)$$

In Fig. 1, we have chosen the negative energy beam wave, α, to interact with the plasma waves. Waves β and γ then grow parametrically. Because the negative energy wave gives up energy, it also grows in amplitude. If the fast beam wave, α', is excited, it decays in amplitude while Waves β and γ grow.

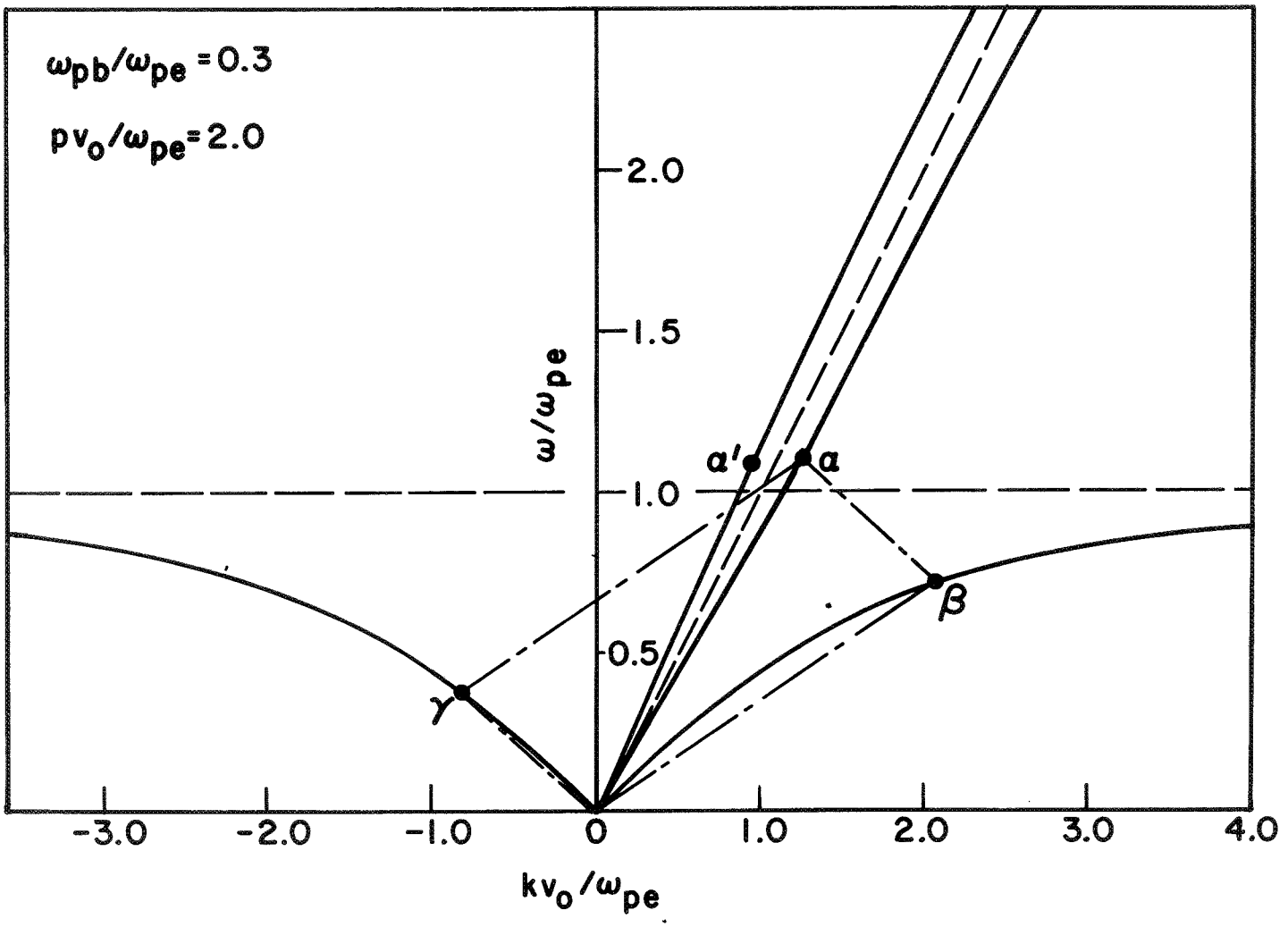

FIG. 1. DISPERSION DIAGRAM OF A STABLE BEAM-PLASMA SYSTEM. WAVES α, β, and γ FULFILL THE SYNCHRONISM CONDITIONS FOR NONLINEAR THREE-WAVE INTERACTION ($\omega_\alpha = \omega_\beta + \omega_\gamma$, $k_\alpha = k_\beta + k_\gamma$)

Figure 2 shows k_α and k_β as a function of ω_α for a few values of the parameter pv_0/ω_{pe}. An increase of the transverse wave number, p, decreases the slope of the plasma wave branch, and thus enhances the stability of the system [see Eq. (51)]. The slow beam space-charge wave is only shown when $pv_0/\omega_{pe} = 1.1$ or 4.0. The other dispersion curves lie between those two. Waves α and β in Fig. 2 interact nonlinearly, since they satisfy Eq. (52). The third wave number, k_γ, is just $k_\alpha - k_\beta$.

4.3. Parametric Growth Rate

Figure 3 shows the relation between the spatial growth rate $|\kappa|$, calculated from Eq. (46) with $Ae\hat{V}_\alpha/mv_0^2$ taken as unity, i.e. for a peak pump amplitude of the order of the beam voltage, and the frequency of the beam wave, ω_α, for the same values of pv_0/ω_{pe} as for Fig. 2. Due to the fact that the group velocities of both plasma waves approach zero when $\omega_\alpha \to 2\omega_{pe}$ and $\omega_\beta, \omega_\gamma \to \omega_{pe}$, we see that $|\kappa| \to \infty$, violating the assumption of a slow space-time dependence of the wave amplitude. We should neglect that part of the diagram anyway, since the assumption of a cold plasma will no longer be valid for large values of k_β and k_γ.

The type of instability described by Fig. 3 is actually absolute. This is so because the plasma waves (β, γ) have opposite group velocities, and it follows from Eq. (39) that $\kappa^2 < 0$. The spatial variation of this three-wave interaction is consequently sinusoidal. As pointed out in connection with Eq. (40), only when the interaction length is short enough does the system exhibit convective instability.

A useful approximation to Eq. (46) for κ is obtained by noting that

$$\Delta_\beta = p^2/k_\beta \quad . \tag{54}$$

Thus we find that $\kappa \propto (k_\beta k_\gamma)^{1/2}$, or alternatively

$$\kappa \propto \left[\left(\omega_{pe} - \omega_\beta\right)\left(\omega_{pe} - \omega_\gamma\right)\right]^{-1/2} \quad . \tag{55}$$

For the higher frequencies, Fig. 3 demonstrates this behavior. From Eq. (55), we note further that the behavior of κ would change little

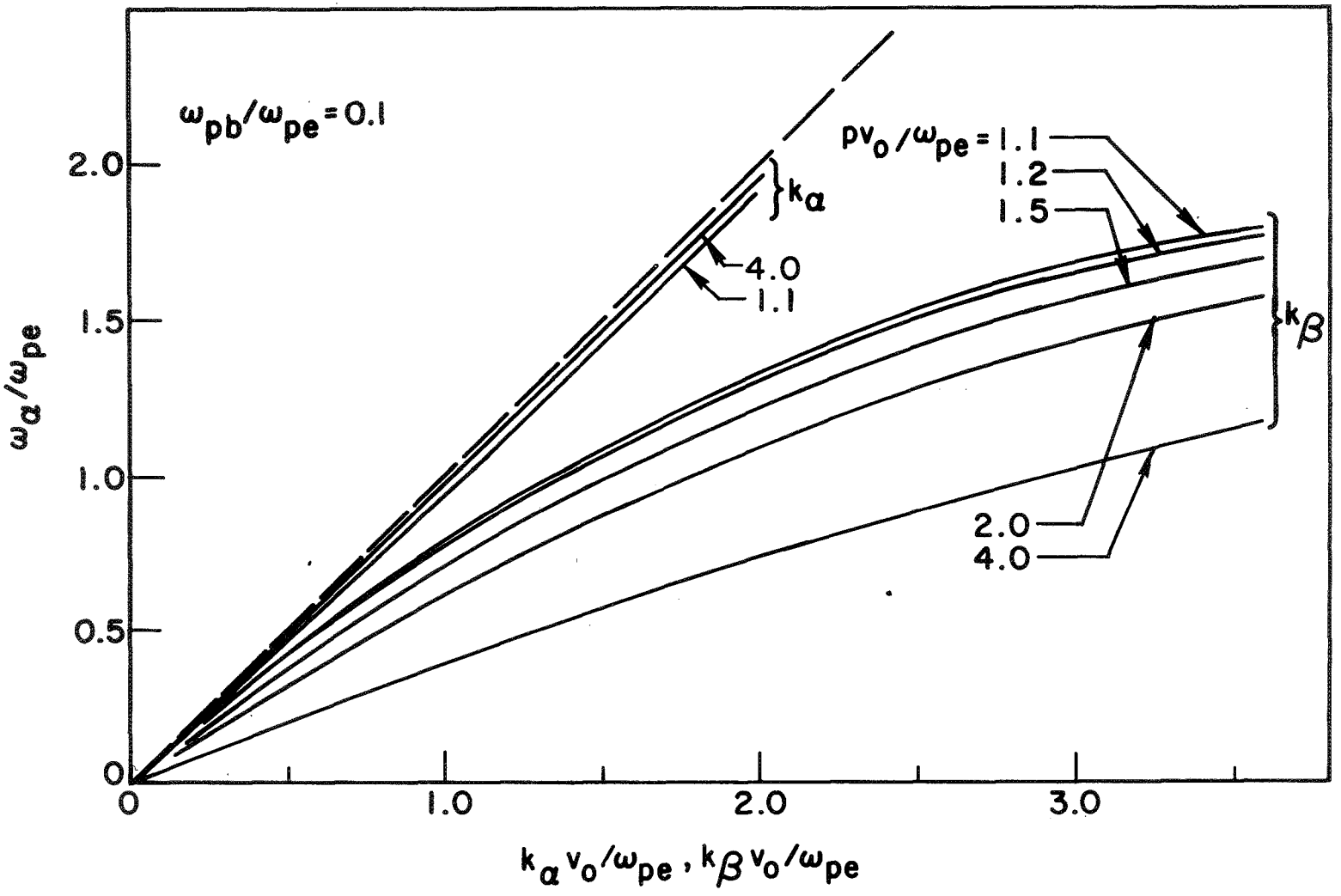

FIG. 2. VARIATION OF THE FREQUENCY OF THE BEAM WAVE, ω_α , AND WAVENUMBERS k_α , k_β , FOR THE NONLINEARLY INTERACTING WAVES OF FIG. 1.

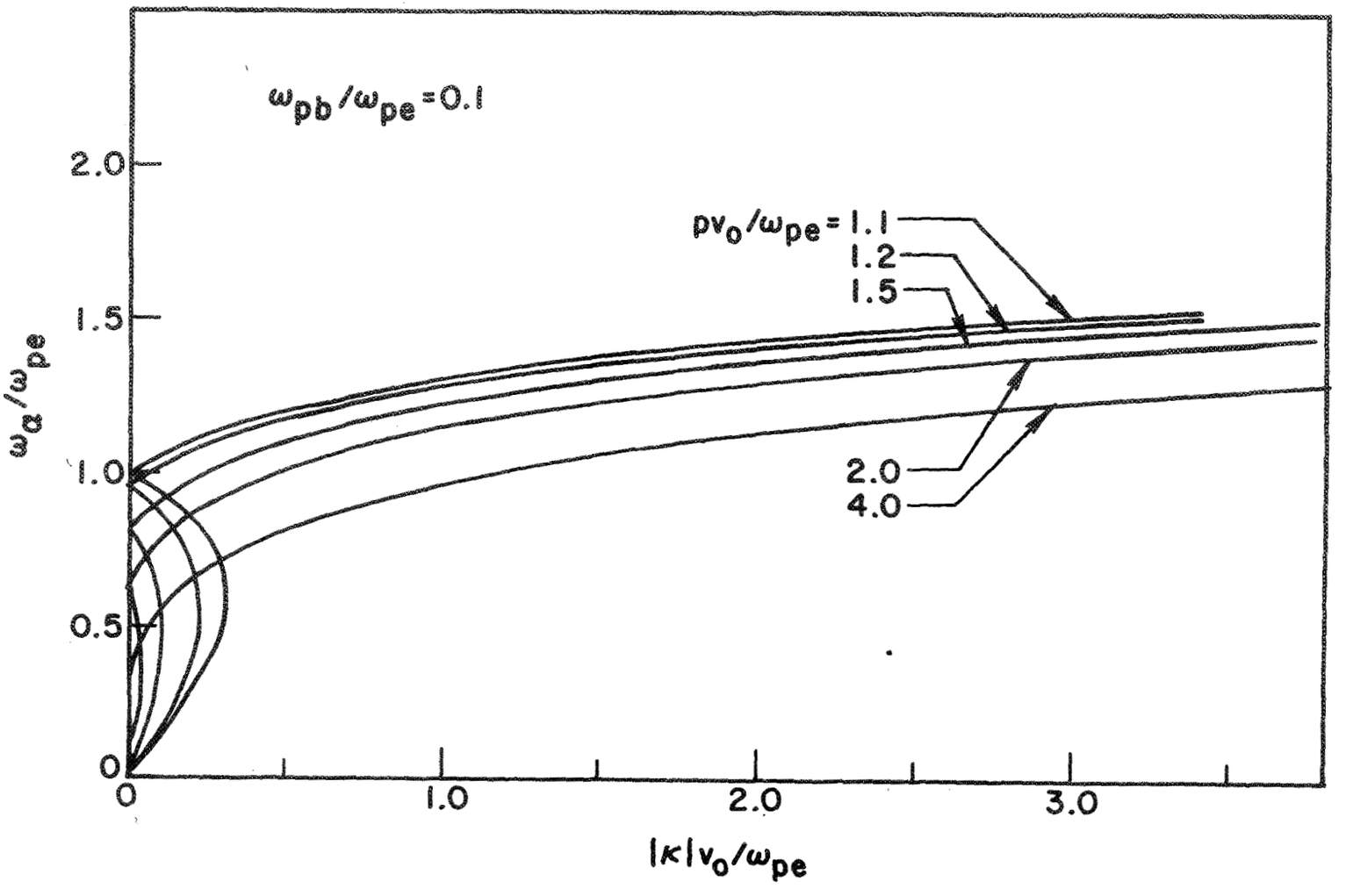

FIG. 3. VARIATION OF ω_α AND THE SPATIAL GROWTH PARAMETER, $|\kappa|$, FOR THE NONLINEARLY INTERACTING WAVES OF FIG. 1: EFFECT OF VARYING pv_0/ω_{pe} (IN THIS CASE, κ IS PURELY IMAGINARY)

if, instead of a beam wave, a plasma wave acted as pump. We would then have

$$\kappa \propto (\omega_{pe} - \omega_{\beta})^{-1/2} \quad . \tag{56}$$

Figure 3 indicates that for some combination of parameters $\kappa = 0$. This point is determined by $\Gamma_{\alpha\beta\gamma}$, which can change sign.

Near the origin of the dispersion diagram, the corresponding value of κ can be approximated by use of Eq. (50). We obtain

$$\kappa \approx - \frac{iA\omega_{\alpha}\,\omega_{pe}}{4p\,v_0^4} \left[1 - 3\,\frac{\omega_{pb}^2}{\omega_{pe}^2}\right] \left|\frac{e\hat{V}_{\alpha}}{m}\right| . \tag{57}$$

for values of p that are not too near to the limiting value expressed by Eq. (51). In agreement with Fig. 3, we find that κ is inversely proportional to the parameter pv_0/ω_{pe}. Its dependence on ω_{pb} is shown in Fig. 4. As Eq. (57) shows, this dependence is rather weak because the beam wave is the pump wave.

So far, we have been discussing calculations of the spatial growth rate. In Figs. 5 and 6, the temporal growth rate is given for the same parameter values as Figs. 3 and 4. From Eq. (36) it is clear that the relation between Ω and κ is

$$\Omega^2 = \kappa^2\, v_{g\beta}\, v_{g\gamma} \ , \tag{58}$$

or alternatively

$$\kappa = i\,\Omega \Big/ \left|v_{g\beta}\, v_{g\gamma}\right|^{1/2} \ , \tag{59}$$

Since $v_{g\gamma}$ is negative. It will be noted from Figs. 5 and 6 that Ω remains finite for all ω_{α}.

The increase in κ and Ω shown by Figs. 3 and 5 when p decreases, and approaches the small-signal stability limit, is an interesting feature. See also Akhiezer et al. [1964], for instance, on this point.

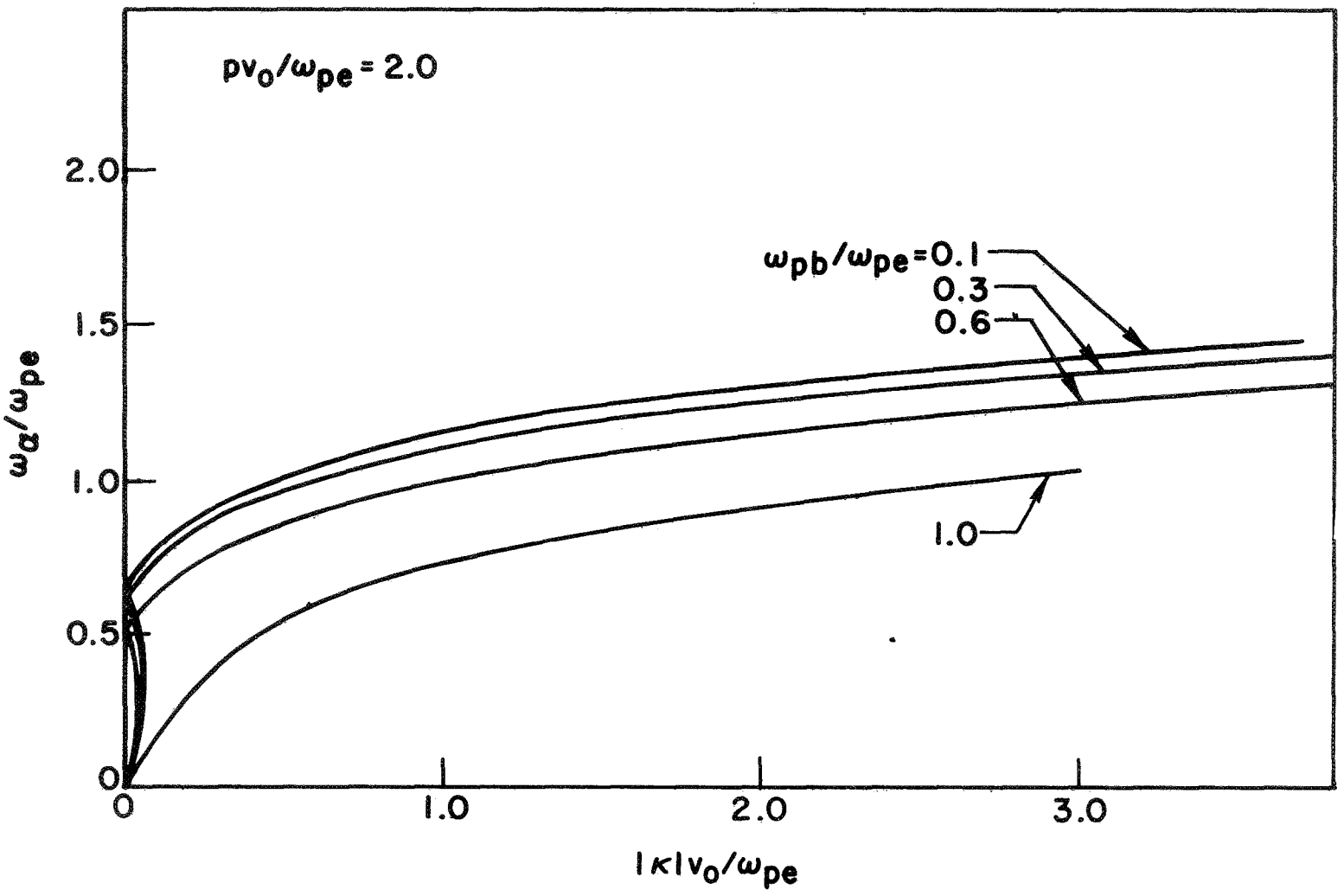

FIG. 4. VARIATION OF ω_α AND THE SPATIAL GROWTH PARAMETER, $|\kappa|$, FOR THE NONLINEARLY INTERACTING WAVES OF FIG. 1: EFFECT OF VARYING ω_{pb}/ω_{pe}

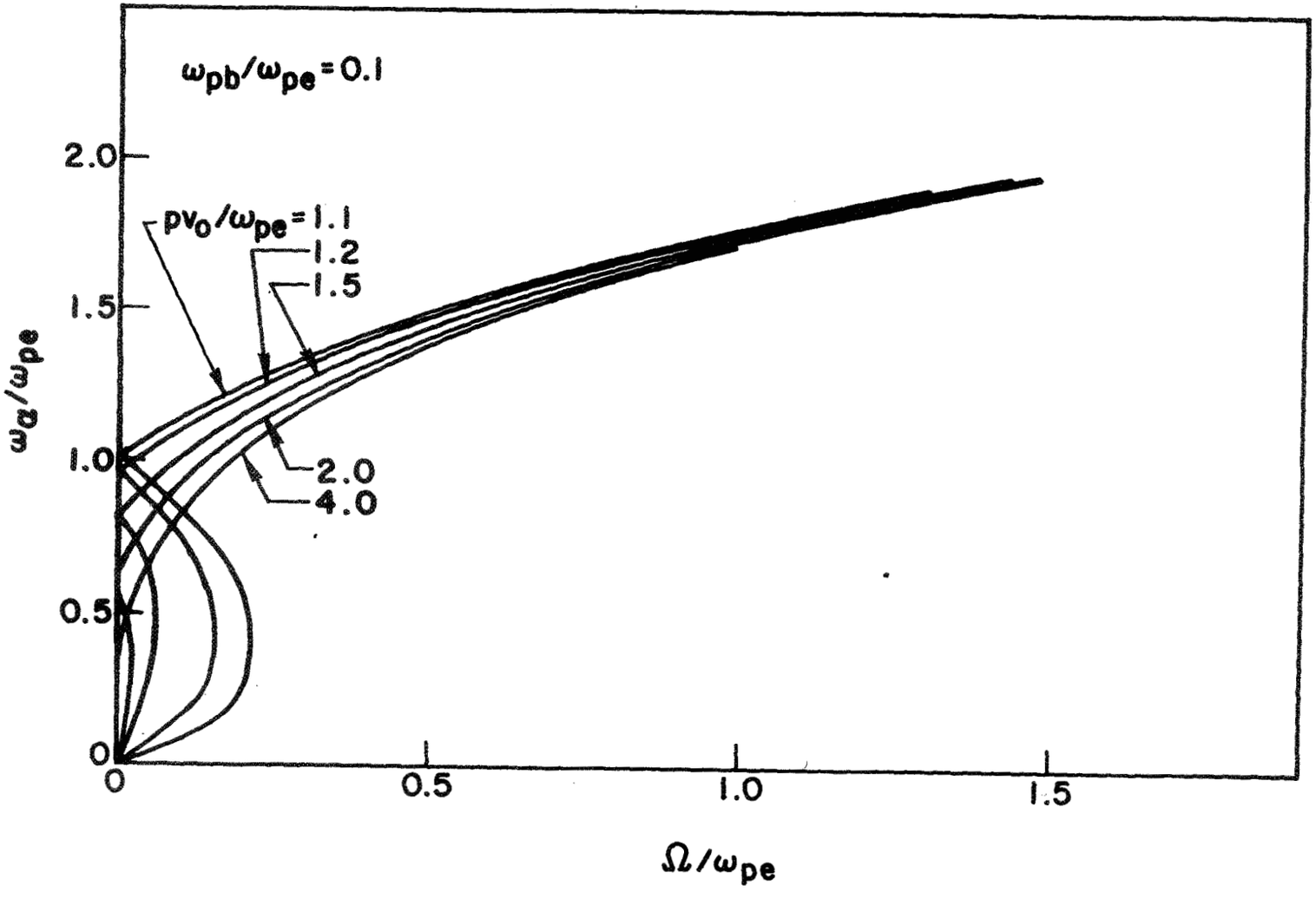

FIG. 5. VARIATION OF ω_α AND THE TEMPORAL GROWTH PARAMETER, Ω, FOR THE NONLINEARLY INTERACTING WAVES OF FIG. 1: EFFECT OF VARYING pv_0/ω_{pe}

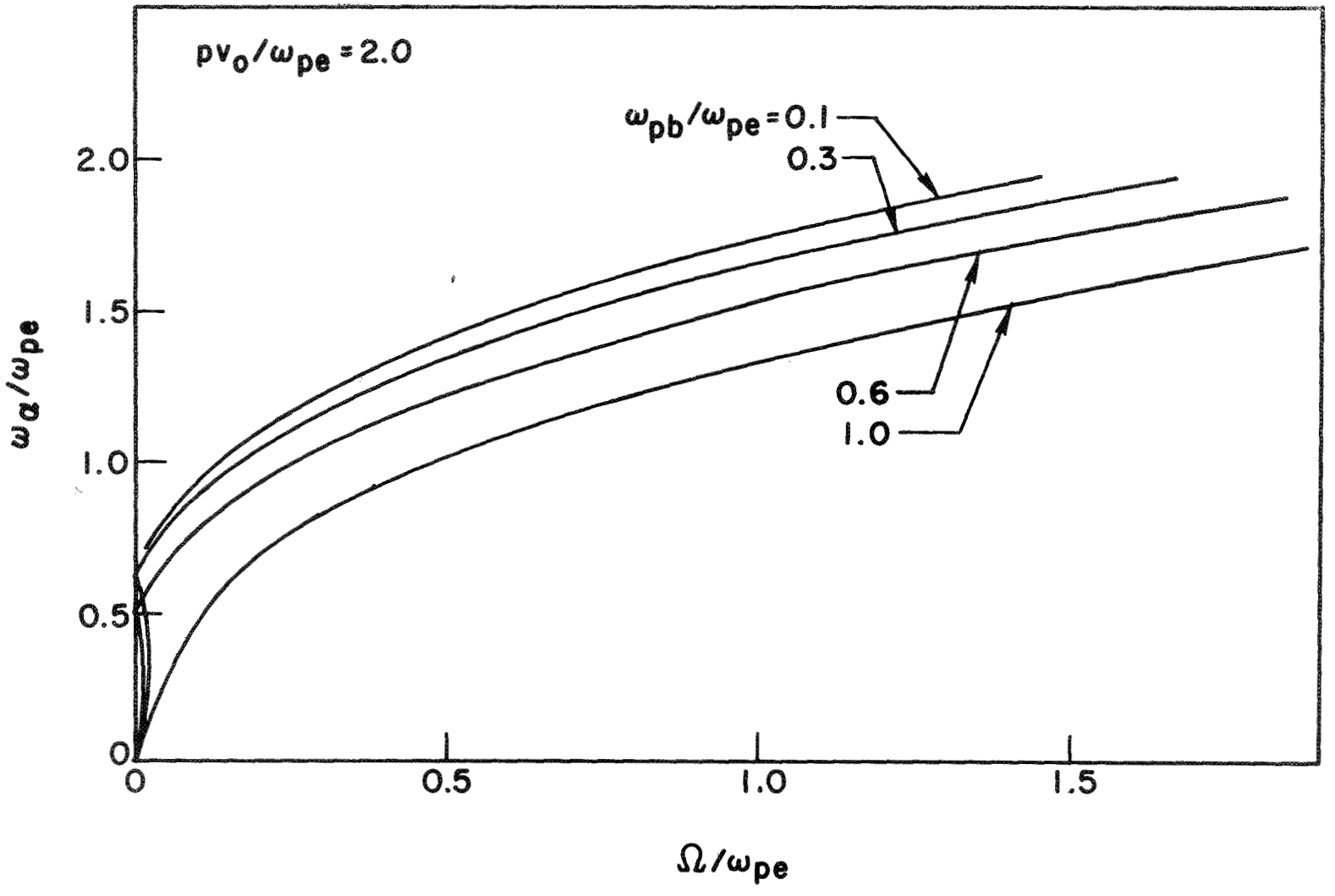

FIG. 6. VARIATION OF ω_α AND THE TEMPORAL GROWTH PARAMETER, Ω , FOR THE NONLINEARLY INTERACTING WAVES OF FIG. 1: EFFECT OF VARYING ω_{pb}/ω_{pe}

4.4. Effect of Positive Ions

Taking into account a third, heavy particle, species does not make any appreciable change in the linear dispersion, obtained by setting $D(\omega,k) = 0$ in Eq. (42). For an ion-electron plasma we obtain

$$1 - \frac{\omega_{pe}^2 + \omega_{pi}^2}{\omega^2} = -\frac{p^2}{k^2} , \tag{60}$$

where ω_{pi}^2 is completely negligible with respect to ω_{pe}^2. As the same is true for $\Gamma_{\alpha\beta\gamma}$, our calculations for κ and Ω are still valid in the three-component system.

There is an implicit assumption in the above remarks, however, that for the ions a one-dimensional approximation is valid. For the experiment to be discussed in Section 5, this is not true. The assumptions of one-dimensionality for the electrons can be expressed by

$$\omega_{pe} \ll \omega_{ce} , \tag{61}$$

where ω_{ce} is the electron cyclotron frequency. As $\omega_{pe} \propto m^{-1/2}$ and $\omega_{ce} \propto m^{-1}$, Eq. (61) is quite compatible with

$$\omega_{pi} \gg \omega_{ci} , \tag{62}$$

and in fact the ions do not fulfill the condition for one-dimensional behavior, in our experiment. The dispersion equation [Eq. (42)] consequently has to be modified, and becomes for a cold ion-electron plasma [Bers 1964]

$$\frac{1 - \dfrac{\omega_{pe}^2}{\omega^2}}{1 - \dfrac{\omega_{pi}^2}{\omega^2 - \omega_{ci}^2}} = -\frac{p^2}{k^2} \tag{63}$$

The result of this is that in addition to the resonance when $\omega \to \omega_{pe}$, the dispersion diagram now shows a cut-off for

$$\omega = \omega_{\ell h} = \left(\omega_{pi}^2 + \omega_{ci}^2\right)^{1/2} \tag{64}$$

When the plasma dispersion branch runs from $k = 0$ to $k = \infty$, it now has to cut the beam dispersion branch. The conclusion is that such a beam-plasma system is always unstable. Under the conditions (61) and (62) it is a low frequency instability, with a small growth rate [Vermeer et al. 1967]. An approximation to Eq. (63) in the neighborhood of $\omega_{\ell h}$ is

$$k^2 = p^2 \, (\omega - \omega_{\ell h}) \, \frac{2\omega_{\ell h}^3}{\omega_{pe}^2 \, \omega_{pi}^2} , \tag{65}$$

and Fig. 7 gives the dispersion of both beam and plasma near $\omega_{\ell h}$, for the same parameters as Fig. 1. The scale factor of 250 by which the variables kv_0/ω_{pe} and ω/ω_{pe} have been multiplied, is approximately $(M_i/m_e)^{1/2}$ where M_i is the mass of an argon atom.

When the beam is modulated, interaction is possible between the beam space-charge waves and the low frequency instability. This is the same type of three-wave interaction as we have been discussing. If the beam wave is again taken to be the pump, and the low frequency instability is the signal wave, then the idler must be a wave that propagates on the beam. In general, there cannot be a complete match of the wavenumbers, however. A small mismatch $\Delta k [= k_\alpha - (k_\beta + k_\gamma)]$ will be introduced because the slope of the beam dispersion branch near the origin is smaller than the slope for high frequencies. This mismatch introduces a factor of $\exp i\Delta kz$ in the second term of Eq. (18). Equation (27) has to be modified slightly and becomes

$$\left\{\frac{\partial}{\partial t} + v_{g\alpha} \frac{\partial}{\partial z} + \gamma_\alpha\right\} \hat{V}_\alpha = 2i \, \frac{\Gamma_{\alpha\beta\gamma} \, \hat{V}_\beta \, \hat{V}_\gamma \, A}{(p^2 + k_\alpha^2) \, \partial D_\alpha / \partial \omega} \exp i\Delta kz \, . \tag{66}$$

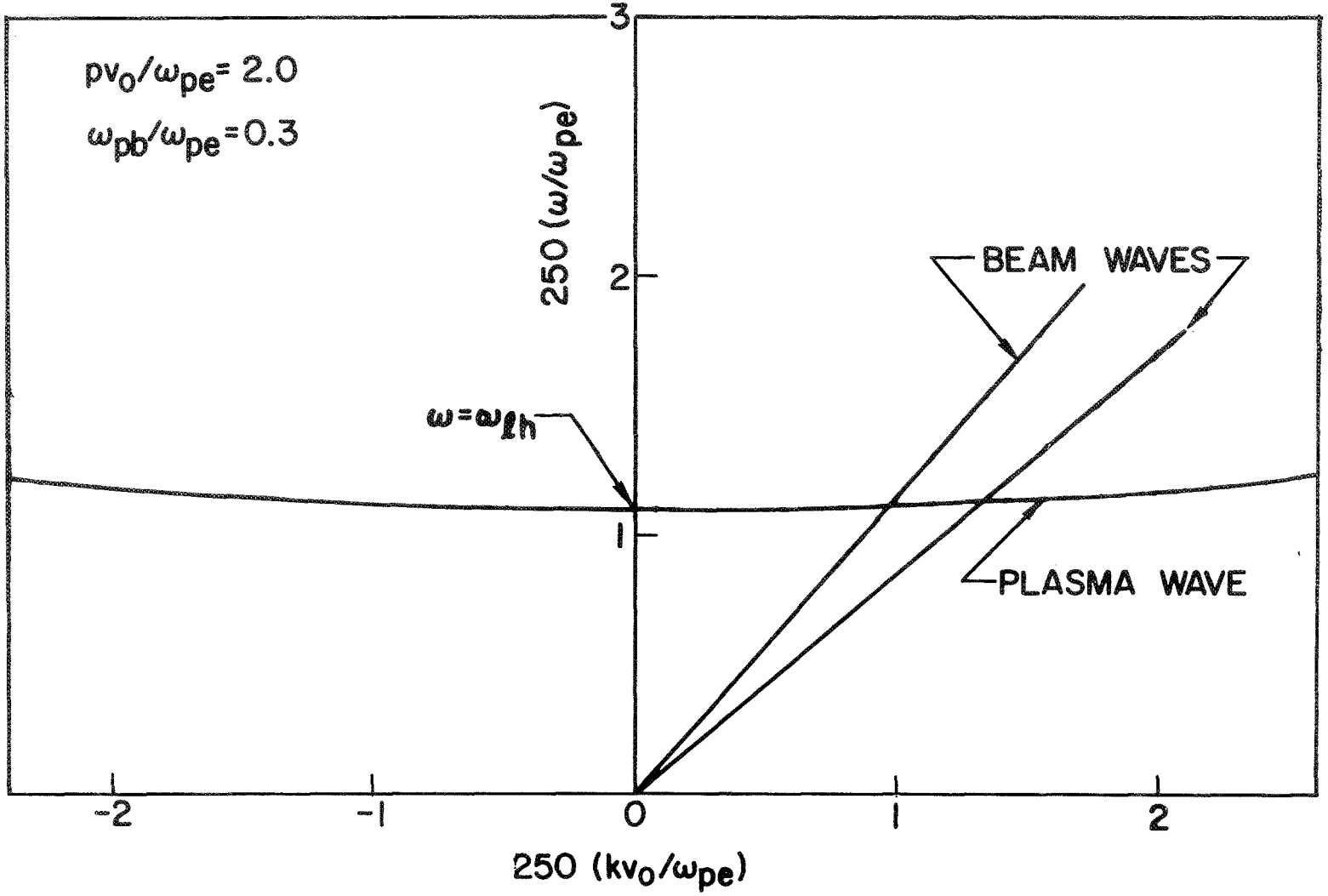

FIG. 7. UNCOUPLED BEAM AND PLASMA WAVE CHARACTERISTICS SHOWING THE CUTOFF OF THE PLASMA WAVE AT THE LOWER HYBRID FREQUENCY, $\omega_{\ell h}$

Considering only spatial dependence, the analogous result to Eq. (35) is

$$\left\{ \frac{\partial^2}{\partial z^2} + i\,\Delta k\,\frac{\partial}{\partial z} \right\} \hat{V}_\beta = \frac{4|\Gamma_{\alpha\beta\gamma}|^2}{\Delta_\beta \Delta_\gamma} |\hat{V}_\alpha|^2 \hat{V}_\beta A^2 \ . \tag{67}$$

From this, we obtain

$$\kappa = -\frac{i}{2}\Delta k \pm \left(\kappa_0^2 - \frac{1}{4}\Delta k^2\right)^{1/2} , \tag{68}$$

where κ_0 is the value for the nonlinear growth in the case of a perfect match, given by Eq. (46). Parametric growth is clearly only possible when $\kappa_0 > \Delta k/2$. Thus, mismatch introduces a threshold, and also an oscillatory spatial dependence of the amplitudes $\hat{V}_\beta$ and $\hat{V}_\gamma$.

An estimate of the mismatch in the wave numbers can be obtained from the dispersion equation for the beam waves in Eq. (49). The low frequency instability is approximated with $k \ll p$, resulting in

$$\omega_{\ell h} = k_{\ell h}\,(v_0 - \omega_{pb}/p) \ . \tag{69}$$

The high frequency waves that propagate on the beam are approximated with $k \gg p$, which gives

$$\omega_\alpha = k_\alpha v_0 - \omega_{pb} \ , \ \omega_\beta = k_\beta v_0 + \omega_{pb} \ . \tag{70}$$

Combining these equations we find

$$\Delta k = 2\,\omega_{pb}/v_0 \ . \tag{71}$$

The mismatch may actually be smaller than $2\,\omega_{pb}/v_0$, because the instability does not occur exactly at $(\omega_{\ell h}\ ,\ k_{\ell h})$, but in a region about this point.

Finally, we calculate the coupling coefficient and the growth rate using the above approximations. From Eqs. (43) and Eq. (46) we obtain

$$\Gamma_{\alpha\beta\gamma} \approx - \frac{e}{2m} \frac{k_\alpha^2 p^2}{\omega_{pb}^2} , \tag{72}$$

$$\kappa \approx iA \left| \frac{e \hat{V}_\alpha}{2m} \right| \frac{k_\alpha p^2}{\omega_{pb}} \left(\frac{k_{\ell h} v_0}{p^3 v_0^3 - \omega_{pb} \omega_{pe}^2} \right)^{1/2} . \tag{73}$$

5. EXPERIMENTAL WORK

In Section 4, two types of nonlinear wave-wave interactions were discussed: first, interaction between a beam space-charge wave and two plasma waves, and second, interaction between two beam space-charge waves and an ion plasma wave. In our experiments, interactions of the first type may have been observed, but the data were very inconclusive. We will therefore only discuss those experiments involving measurements of the second type of interaction.

5.1. Experimental Set-up

Figure 8 shows the set-up used. Detailed descriptions of it have already been given elsewhere (see reference to Forrest et al. 1969). The electron gun gave typically a beam of 20-50 V, 0.5-5.0 mA, which created a low density plasma in the neutral background of argon at 10^{-6} - 10^{-4} Torr. The plasma and beam were immersed in an axial magnetic field of about 500 G, spatially homogeneous to within ± 1.5 per cent.

For launching and detecting waves in the plasma or on the beam, two probes were available together with the inner grid in the gun. One probe was fixed in axial location, and could be moved radially. The other could be moved along the plasma column. Its stem passed to the outside through a Wilson seal, and had the defect of causing pressure variations when it was moved, especially when it was moved inward. The outer grid of the gun was at ground potential, as was the plasma chamber. The inner grid was connected to a variable voltage supply and served to regulate the extracted beam current. It was also connected capacitively to the outside, and proved to be a much more efficient detector of plasma waves than a probe. The beam voltage was determined by the setting of the gun cathode voltage.

Connection of the inner grid to a spectrum analyzer demonstrated that the gun region was very noisy. The strength of the noise depended sensitively on the dc voltage on the inner grid. Under some conditions, parts of the gun noise spectrum were found to propagate into the plasma. Generally, it was found that a quiet gun region was associated with a beam-generated plasma with only a small axial density gradient.

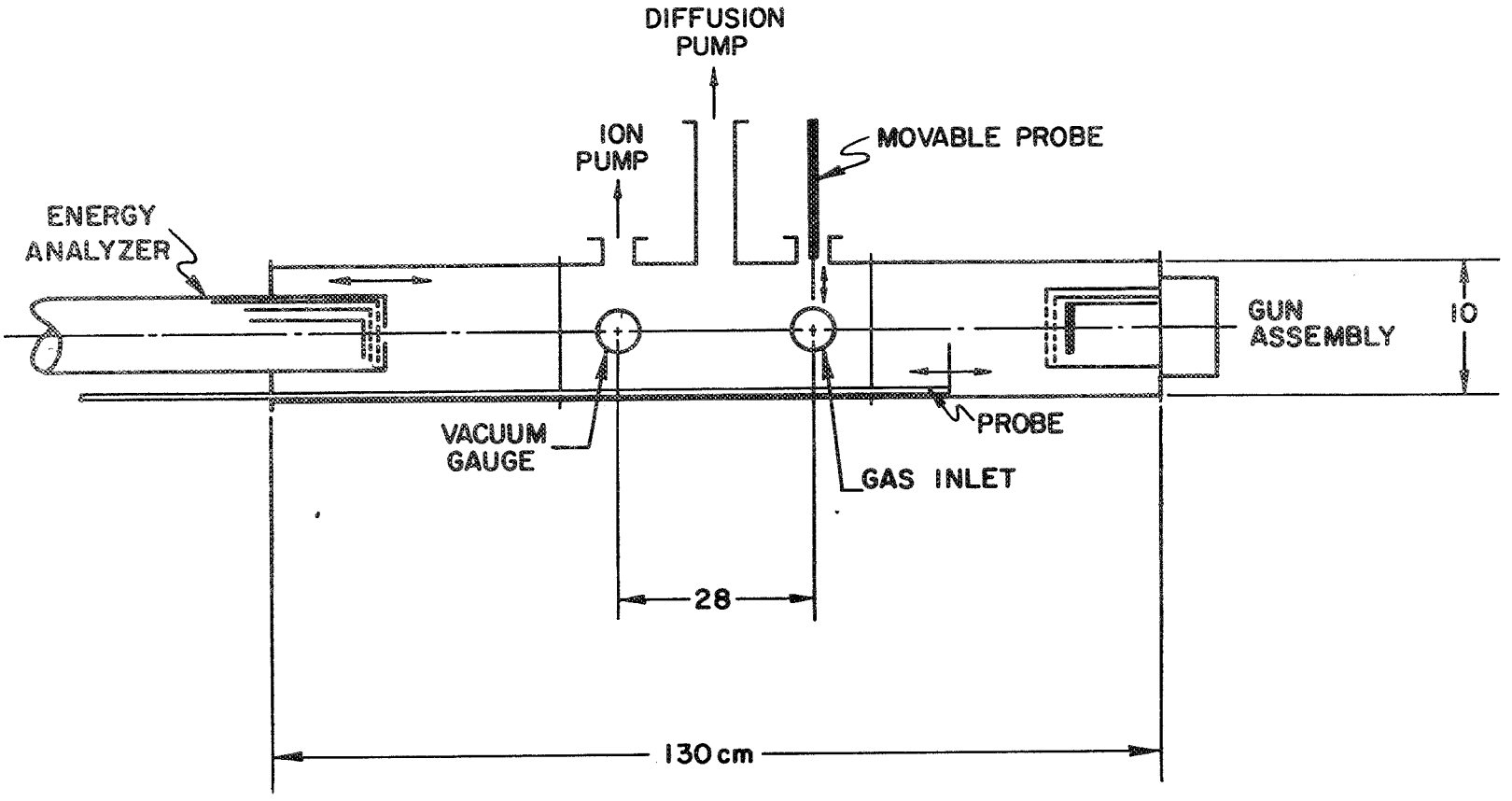

FIG. 8. EXPERIMENTAL SET-UP

To avoid strong reflection of waves from the end of the plasma tube, a graphite cone was mounted on the energy analyzer.

5.2. The Plasma Parameters

A powerful method of determining beam and plasma parameters is to measure the wave dispersion characteristics of the system. The conventional set-up used to measure the relevant phases and amplitudes is illustrated in Fig. 9. Cables A and B could be connected to either of the probes, or to the inner grid of the gun. The detector set-up as a whole was accurately square-law.

It should be emphasized that some care is needed to use the particular situation depicted in Fig. 9. Since the grid is 10 - 20 dB more effective in launching waves than is a probe, the oscillator signal must not be allowed to leak through the hybrid junction and the variable attenuator to the gun. By connecting a probe to a spectrum analyzer, it was checked that any beam modulation due to this effect was below the detection level used in the measurements.

Another source of concern was secondary emission from the probes, caused by beam bombardment. It was found that signals carried by the resulting streams of secondary electrons could be more pronounced than those propagating through the plasma. For this reason, the exciter probe was not allowed to penetrate into the beam.

Referring to Fig. 1, we see that a high frequency signal excites the two beam waves: the slow beam space-charge wave with wave number k_s, and the fast wave, k_f. These waves will interfere and produce a spatial amplitude pattern in the plasma tube, with a wave number k_i $[=(k_s - k_f)/2]$. For large k, $k_i \approx \omega_{pb}/v_0$, so that measurement of this quantity gives ω_{pb} directly.

To measure the plasma dispersion characteristics, it is preferable to excite with a probe Wave γ in Fig. 1, propagating towards the gun with a negative phase velocity. In the other direction, three waves are excited, one plasma wave and two beam waves. These give a doubly periodic interference pattern in the plasma, and correspondingly complicated measurements to interpret. Typical phase and amplitude measurements on Wave γ are illustrated by the inset in Fig. 10. In this case, the wave

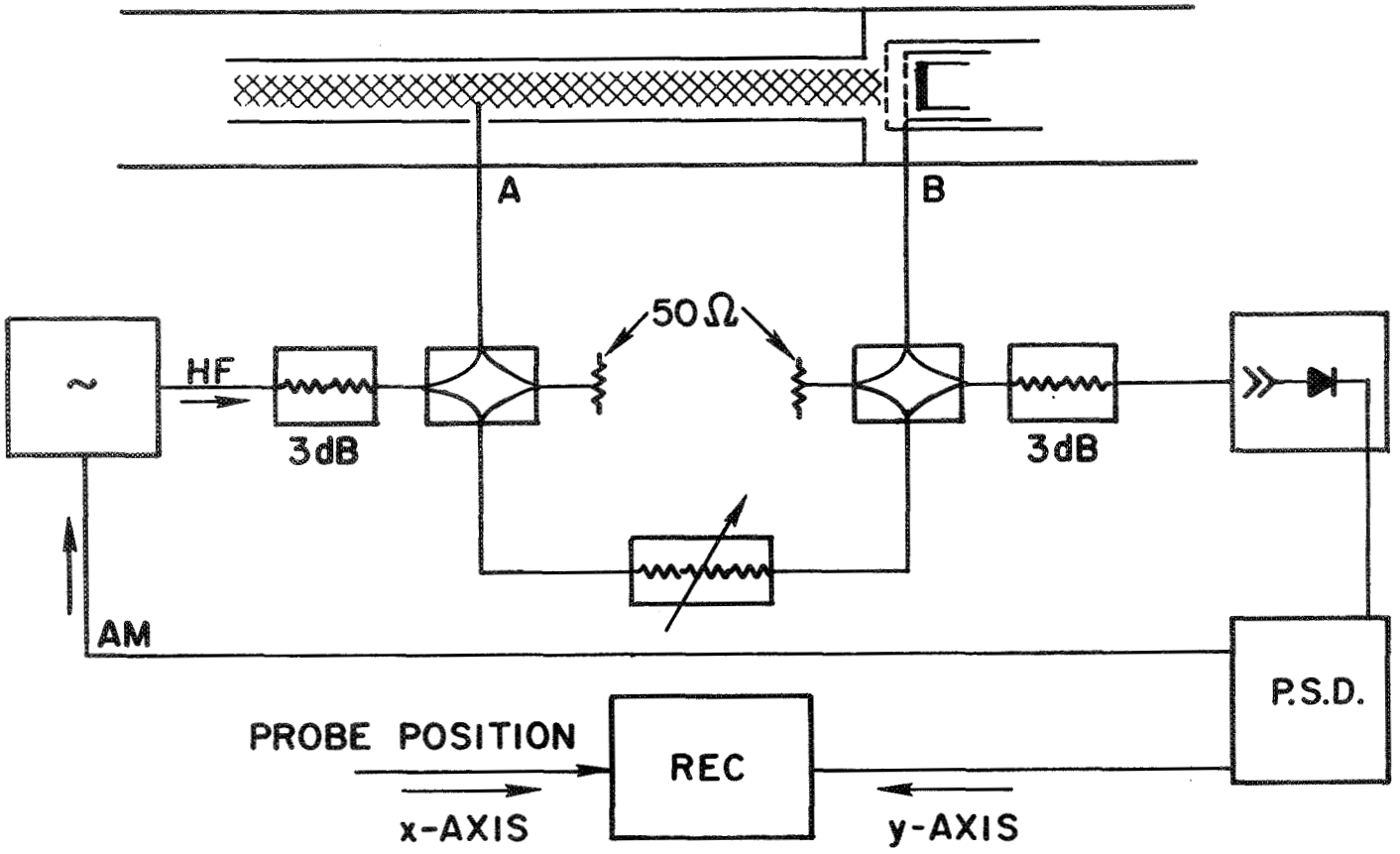

FIG. 9. MICROWAVE INTERFEROMETER

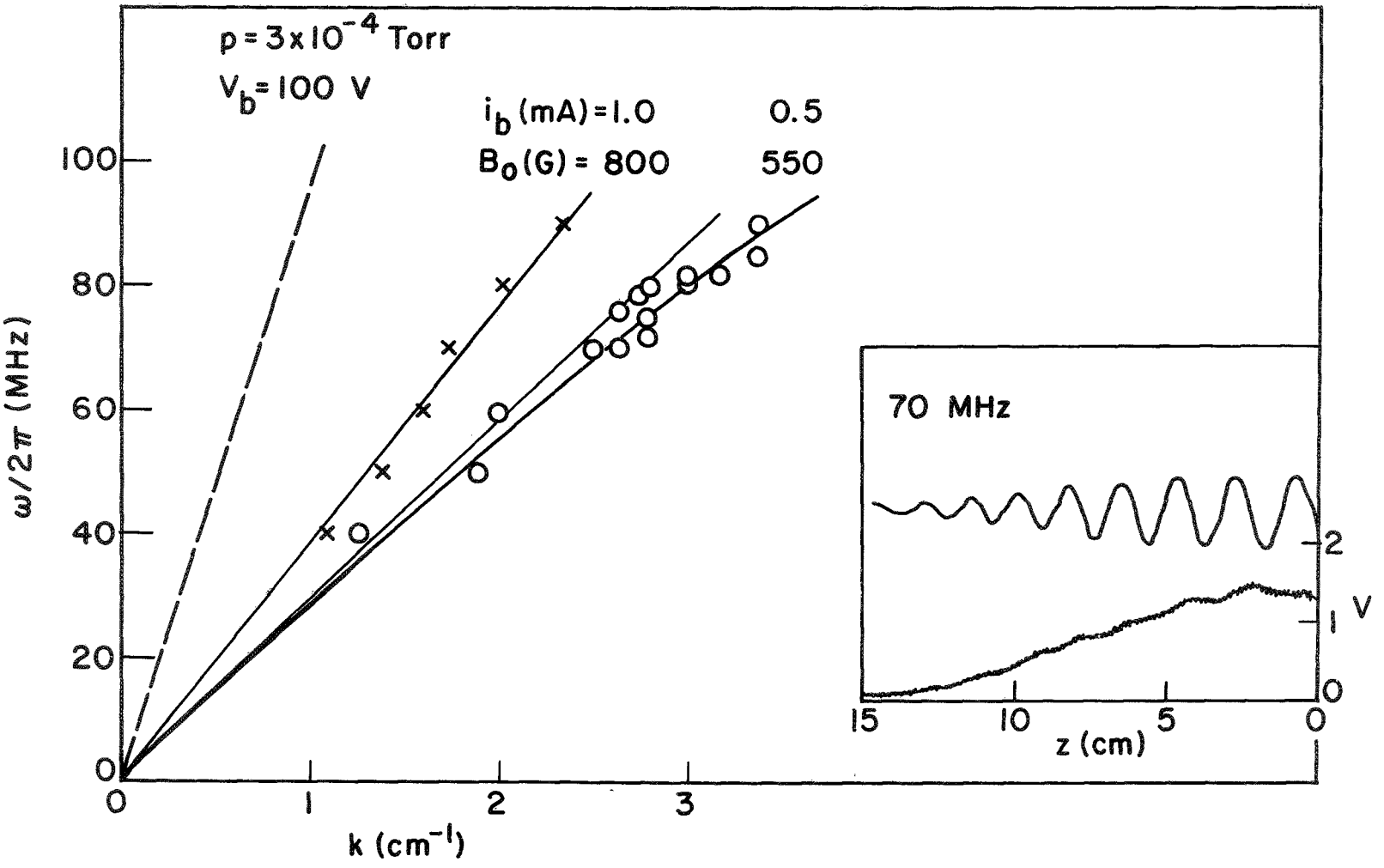

FIG. 10. DISPERSION OF PLASMA WAVE PROPAGATING TOWARDS THE GUN (Wave γ OF FIG. 1). (THE DASHED LINE INDICATES THE DISPERSION OF THE BEAM SPACE-CHARGE WAVES. TYPICAL MEASUREMENTS OF PHASE AND AMPLITUDE ARE SHOWN INSET FOR i_b = 1.0 mA, AND FIRST GRID VOLTAGE = -40 V)

is launched by the axial probe, and detected by the gun grid. Some dispersion diagrams resulting from such measurements are shown in Fig. 10. The beam plasma frequency is about 2 MHz in the 0.5 mA case, and the beam dispersion curves fall closely around the dashed line. The slope of the plasma dispersion curve is $\omega_{pe}/2\pi p = 29 \times 10^6$ cm^{-1} [see Eq. (47)], and the full theoretical dispersion curve [Eq. (44)] fits through the measured points for $\omega_{pe}/2\pi \approx 200$ MHz and $p \approx 7$.

Figure 10 demonstrates that it is feasible to achieve experimental dispersion characteristics that should be linearly stable in the high frequency region. It was checked independently with a spectrum analyzer, that the plasma was indeed stable. As can be anticipated from the discussion in Section 4.4, the system is still unstable in the low frequency range (below 1 MHz) at frequencies that are approximately equal to $\omega_{pe}\left(m_e/M_i\right)^{1/2} = \omega_{pi}$, with $\omega_{ci} \ll \omega_{pi}$, $\omega_{\ell h} \approx \omega_{pi}$.

To make the system more stable, and to increase the range over which the experimental parameters could be varied, the plasma was surrounded by a slotted stainless steel tube 38 cm in diameter and 40 cm long, as indicated in Fig. 9. The dispersion characteristics shown in Fig. 10 were measured in this tube. Due to the gap between the tube and the gun, the plasma is inhomogeneous over the first 2 cm, and is useless for measurements. This is illustrated by the data inset in Fig. 10 which show an anomalous amplitude increase over these 2 cm, compatible with a strong density decrease. The plasma homogeneity was checked further by using the axial probe as a negatively-biased Langmuir probe, measuring the ion saturation current, i_+. Within the narrow tube, i_+ changed by ± 2 per cent, with a probe voltage of -20 V. Similar results were obtained with a floating probe.

Some observations were made of the floating potential. This was found to be about 1.9 V, and varied by less than 1 per cent, except over the first 3 cm, where its value might jump irregularly by a factor of ten.

Fluctuation levels in the beam current could be measured with the energy analyzer shown in Fig. 8. The 60 Hz level varied between 0.5 and 3 per cent, decreasing with increasing gas pressure. Fluctuations in the kHz range were weaker by a factor of about ten.

It is appropriate to emphasize at this point that the experimental studies described here should be regarded as exploratory rather than complete, and that the measurements presented here pose problems which have not yet been resolved. Two of them are suggested by Fig. 10. The first is the very large experimental value of $p \approx 7$, which is to be compared with the value of $p \approx 1.3$ to be expected from Eq. (13) for excitation of the lowest radial mode in a tube with 1.9 cm radius. The second unexplained phenomenon is the very rapid linear damping of the wave amplitude. Since $\omega \ll \omega_{pe}$, this cannot be attributed to Landau damping. Since $p \approx 10^{-4}$ Torr, it cannot be attributed to collisional damping either. Phase mixing due to density fluctuations is a possible contributing factor (see below), but does not seem adequate to explain the observed strength of the damping. Whatever its origin, this damping has the undesirable effect of inhibiting measurements on plasma dispersion above 100 MHz in the 0.5 mA case, when the phase measurement is limited to two fringes or less.

5.3. Three-wave Interaction

Under certain conditions, which depend very sensitively on the beam voltage and gas pressure, the lower hybrid instability described in Section 4.4 is excited and shows a clearly defined spectrum. The peak amplitude is largest for $p \approx 10^{-5}$ Torr and $V_b \approx 20$-50 V. With beam velocity $v_0 \gtrsim 10^8$ cm/s and $\omega_{pi}/2\pi \approx 100$ kHz, the expected wavelength is about 10^3 cm, which is large compared to the length of the apparatus. Experimentally, the oscillations were found to be effectively in phase, i.e. phase differences along the plasma column of less than 30° were measured. The amplitude of the oscillations were observed to be constant in space and in time, implying that the instability was saturated. The amplitude of the fluctuations in the ion saturation current to a probe could be as high as 10 per cent of the total current. The instability frequency was near the ion plasma frequency. Below $p = 10^{-5}$ Torr, the frequency was found to be proportional to the beam plasma frequency, and above 10^{-5} Torr, when an electron plasma is formed, the frequency was proportional to gas pressure. Furthermore, the instability was noted to be independent of magnetic field. These facts together provide strong evidence that the lower hybrid instability was indeed being excited.

The instability was sensitive to changes in v_0 . This was manifested by the narrow peak in the low frequency spectrum becoming a broad noise band for small changes in v_0 . Under conditions when the low frequency spectrum was relatively clean, the three-wave interaction with two beam space-charge waves could be observed readily: Modulating the beam at some high frequency caused sidebands to appear on both sides that are exactly displaced by the frequency of the low frequency instability. Fig. 11 shows an example. It was checked by means of a low frequency spectrum analyser that beam modulation did not have any controlling influence on the low frequency instability, nor did it influence the homogeneity of the plasma, discussed in the previous section. The sidebands at double the low frequency in Fig. 11 demonstrate a coupling between two beam waves, and a low frequency component that is excited independently at about $2\,\omega_{\ell h}$. Figure 12 shows the growth in space of all waves involved in the coupling.

Summarizing, the following properties were verified by our experiments. First, the frequency and amplitude of the sidebands relative to the center frequency were independent of the modulation amplitude for source powers between -15 dBm and + 7 dBm. Second, the amplitudes and frequencies of the sidebands were independent of modulation frequency. Third, the relative amplitudes of the sidebands increased with gas pressure and decreased with beam velocity.

5.4. Discussion

Although, in view of the incomplete nature and understanding of our measurements commented on above, the results presented here should be regarded only as preliminary, Fig. 12 does provide suggestive evidence that the three-wave coupling indeed leads to an "explosive" type of instability in which all three waves grow in amplitude to saturation. The growth does not seem to be due to the linear instability of the beam waves for the following three reasons. First, the growth occurs when the beam is modulated at a frequency above the plasma frequency. Second, the system is stable in the high frequency region, as shown in Fig. 10. Third, the lower hybrid instability only shows spatial growth when the beam is modulated. Under conditions for which the coupling shows up clearly,

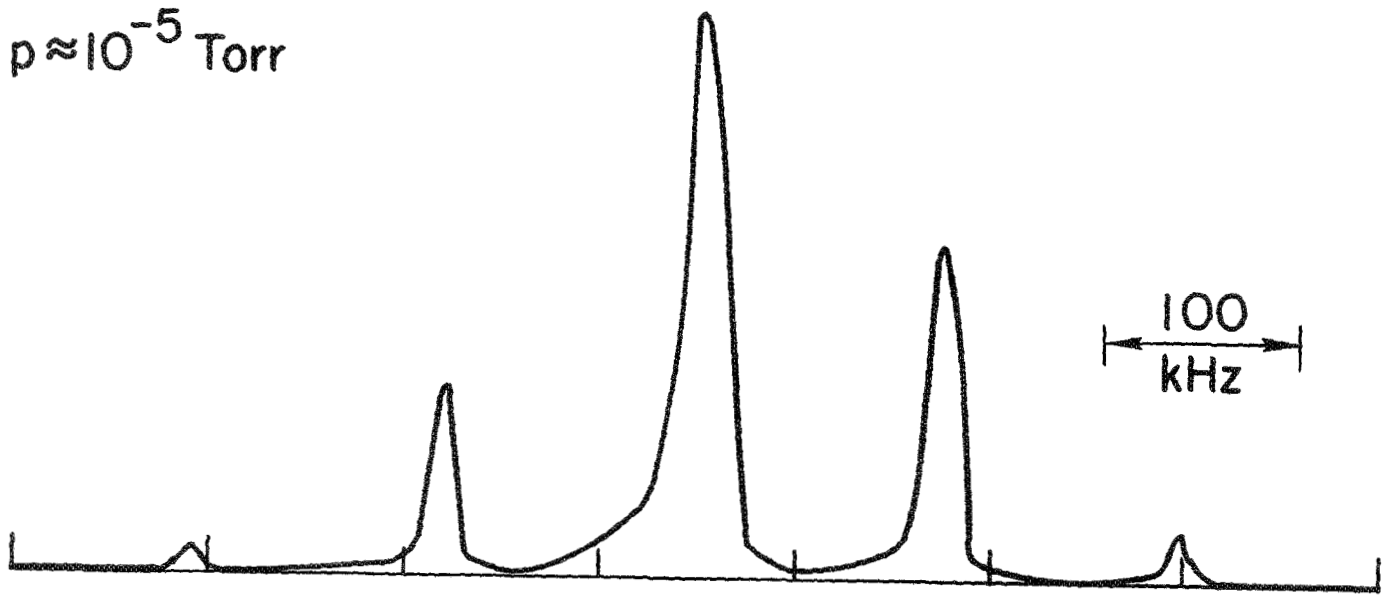

FIG. 11. FREQUENCY SPECTRUM IN THE BAND AROUND THE BEAM MODULATION FREQUENCY. ($p = 10^{-5}$ TORR, $V_b = 100$ V, $i_b = 1.7$ mA, MODULATION FREQUENCY IS 230 MHz. DETECTION IS LINEAR)

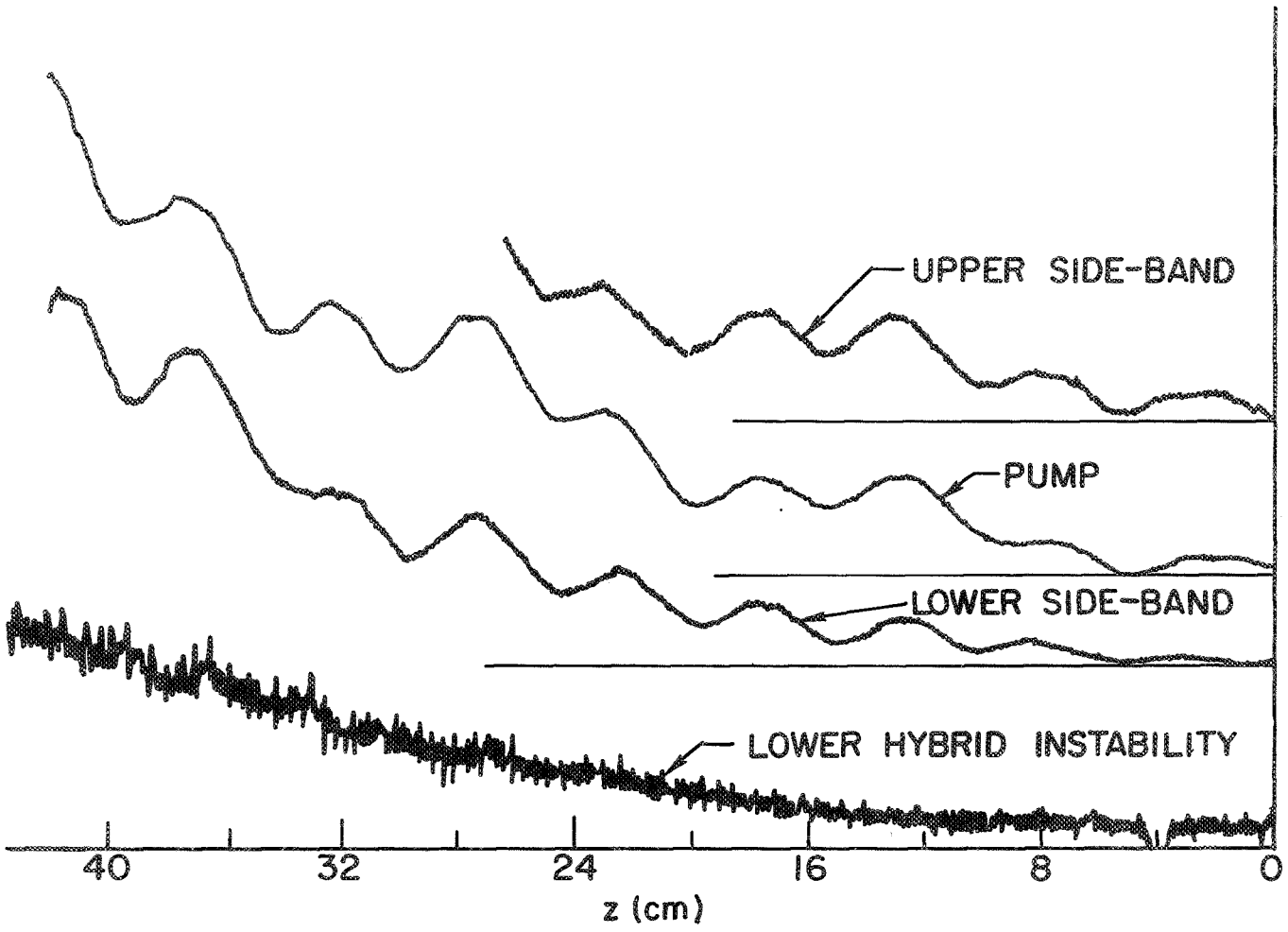

FIG. 12. SPATIAL GROWTH OF THE THREE WAVES INVOLVED IN THE NONLINEAR COUPLING ($p = 2 \times 10^{-5}$ TORR, $V_b = 50$ V, $i_b = 2.5$ mA. DETECTION IS LINEAR. INSTRUMENT BANDWIDTH IS 10 kHz. THE LOWER HYBRID INSTABILITY IS AT 80 kHz. THE SENSITIVITY OF THE RECORDER VARIES FOR THE FOUR TRACES)

there is no indication of a threshold for the instability to occur. Such a threshold might be caused by wave damping or by a mismatch in the wave numbers. The wavelength of amplitude oscillations due to the mismatch is calculated from Eqs. (68) and (69) as $2\pi v_0/\omega_{pb} \approx 100$ cm. We see that this is of the order of the length over which the growth is measured, so the mismatch may be neglected.

With the aid of Eq. (70), the nonlinear growth for parametric excitation of the sidebands is found to be

$$\kappa \approx 10^{-1} \, |V_\alpha| \ \text{cm}^{-1} \qquad (V_\alpha \text{ in volts}) \ , \tag{74}$$

where $|V_\alpha|$ is the amplitude of the pump wave. Replacing the wave numbers by frequencies we find that

$$\kappa \propto \omega_{pe}^{1/2} / v_0^{5/2} \ . \tag{75}$$

This relation is found to hold qualitatively for the interaction of beam waves with a low frequency wave. With a modulation frequency of 80 MHz in Fig. 12, the wavenumber of the beam wave $k_\alpha \approx 1.3 \ \text{cm}^{-1}$, whereas the experimental growth rate $\kappa \approx 0.07 \ \text{cm}^{-1}$. A direct comparison with the calculated growth rate is not yet possible, however, as it is difficult to work in a range where the parametric formulas are valid.

The coupling must be different in the two cases of the lower and the higher frequency sidebands. The Manley-Rowe relations expressed by Eq. (2) demand that the wave with the highest frequency be a negative energy wave for explosive growth to occur. As modulation at the gun excites both beam waves, the low frequency instability apparently interacts with both of them. Coupling with the fast beam wave would result in the upper frequency sideband being a slow beam wave, while coupling with the slow beam wave would result in the lower frequency sideband being a fast beam wave.

Acknowledgement

The author is indebted to Dr. K. B. Dysthe for fruitful discussions on the subject of three-wave interactions, and would like to express his sincere gratitude to Professor F. W. Crawford for giving him the opportunity to work at Stanford University.

REFERENCES

I. A. Akhiezer, I. A. Daneliya, and N. L. Tsintsadze, Sov. Phys.-JETP 19, 208 (1964).

C. W. Barnes, Proc. IEEE 52, 64 and 296 (1964).

H. L. Berk, and D. L. Book, Phys. Fluids 12 649 (1969).

R. J. Briggs, Electron-Stream Interaction with Plasma (MIT Press, Cambridge, Mass., 1964).

C. T. Dum, and E. Ott, Cornell University Report, LPS 38 (1970).

K. B. Dysthe, Int. J. Elect. 29, 401 (1970).

C. Etievant, I. Fidone, and M. Pérulli, Plasma Phys. 9, 151 (1967).

H. E. Fettis, J. Math. and Phys. 36, 88 (1957).

J. R. Forrest, S. Roth and M. Seidl, Stanford University Institute for Plasma Research Report No. 334 (1969) [See also SU-IPR Report No. 355 (1970)].

J. Fukai, S. Krishan, and E. G. Harris, Phys. Rev. Letters, 23, 910 (1969).

A. Hasegawa, R. Davidson, and R. Goldman, Appl. Phys. Letters, 14, 325 (1969).

H. J. Hopman, Proc. IXth International Conference on Phenomena in Ionized Gases, Bucharest, Rumania 1969 (Acad. Soc. Rep. Rumania, Bucharest) [In press].

G. Laval, R. Pellat, and M. Pérulli, Plasma Phys. 11, 579 (1969).

R. Leven, Beitr. Plasma Phys. 3, 169 (1963).

J. Olivain, and M. Pérulli, Proc. VIIIth International Conference on Phenomena in Ionized Gases, Vienna, Austria, (IAEA, Vienna, 1967), p. 398.

Pham-Tu-Manh, Proc. Third European Conference on Controlled Fusion and Plasma Physics, Utrecht, Netherlands, 1969 (Wolters-Noordhoff Publishing, Groningen 1969), 34.

R. Z. Sagdeev, and A. A. Galeev, Nonlinear Plasma Theory, (W. A. Benjamin New York, N. Y., 1969).

E. N. Spithas, and W. M. Manheimer, Phys. Fluids 13, 1110 (1970).

T. H. Stix, Theory of Plasma Waves (McGraw Hill Book Co., New York, N. Y., 1962).

P. A. Sturrock, Proc. Sixth Annual Lockheed Symposium on Magnetohydrodynamics (Stanford Univ. Press, Stanford, Calif., 1962), p. 47.

A. W. Trivelpiece, Slow Wave Propagation in Plasma Waveguides, (San Francisco Press, San Francisco, Calif., 1967).

H. Wilhelmsson, Proc. Third European Conference on Controlled Fusion and Plasma Physics, Utrecht, Netherlands 1969 (Wolters-Noordhoff Publishing Co., Groningen 1969)

A. Vermeer, T. Matitti, H. J. Hopman, and J. Kistemaker, Plasma Phys. 9, 241 (1967).